Supplement of Nat. Hazards Earth Syst. Sci., 20, 2681–2699, 2020
https://doi.org/10.5194/nhess-20-2681-2020-supplement
© Author(s) 2020. This work is distributed under
the Creative Commons Attribution 4.0 License.

Natural Hazards and Earth System Sciences
Open Access
EGU

Supplement of

Multivariate statistical modelling of the drivers of compound flood events in south Florida

Robert Jane et al.

Correspondence to: Robert Jane (r.jane@ucf.edu)

The copyright of individual parts of the supplement might differ from the CC BY 4.0 License.

Measuring stations

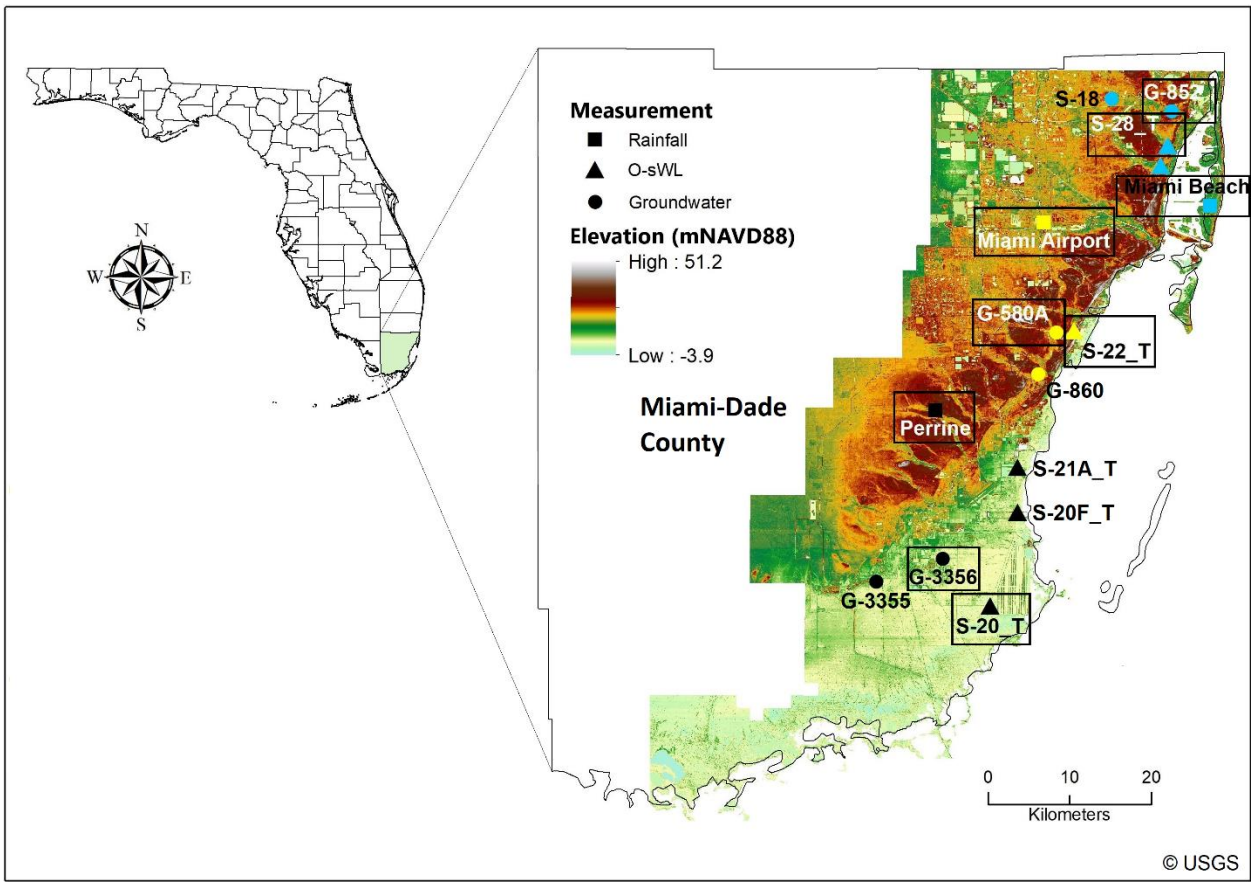

Figure S1: Map detailing the names of all the measuring stations used in the study. Secondary measuring stations i.e. those used only for filling in missing values at the principal stations are not named in the report but are referred to later in this document. Boxes signify the three principal measuring stations – to whose imputed records statistical models are applied - for each of the three case study sites.

Gap length	Frequency
1	3
2	1
3	1
4	1
5	2
6	4
15	1
29	1
38	1
41	2
73	1
176	1
365	1

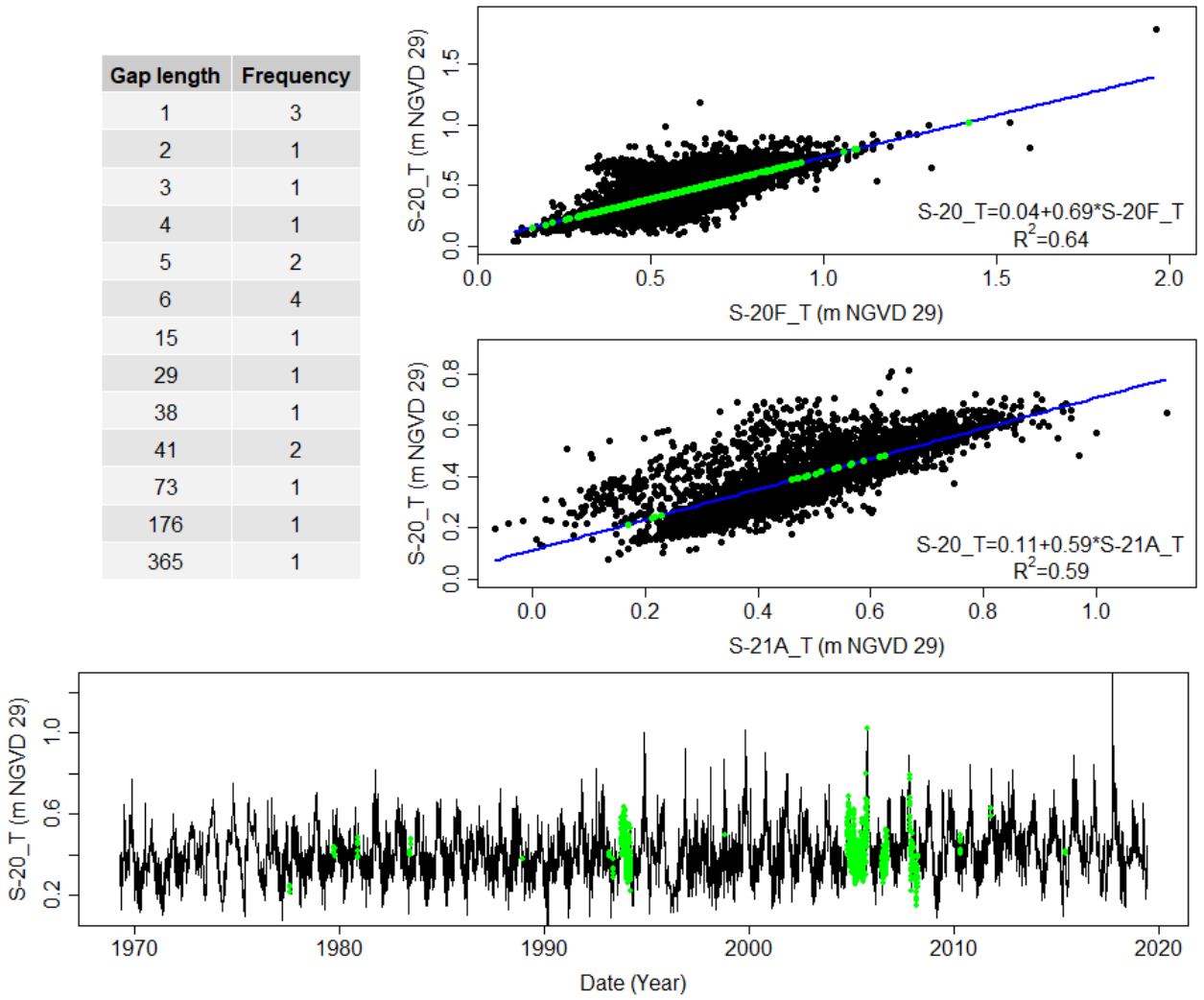

Figure S2: Record at S-20_T - O-sWL at case study site S20 - is imputed using readings first from station S-20F_T with all the remaining missing readings subsequently imputed using the record at station S-21A_T. Linear interpolation was not required to impute missing values at this station.

Upper Left: Table listing the length of consecutive missing value series in the record and the frequency of these gap lengths. For instance, the bottom row of the Table above implies there is one year in the record where every value is missing.

Upper right: Linear regression (blue line) of the observations at the site of interest on those at neighboring station. Black dots are simultaneously occurring observations from the two sites to which the model is fitted, while the green dots denote the missing values at the site of interest, predicted using the regression model.

Lower: Completed time series, identifying the values imputed through linear regression (green dots) and linear interpolation (yellow dots).

Gap length	Frequency
1	13
2	2
3	3
4	1
5	2
8	1
9	1
13	1
34	1
39	1

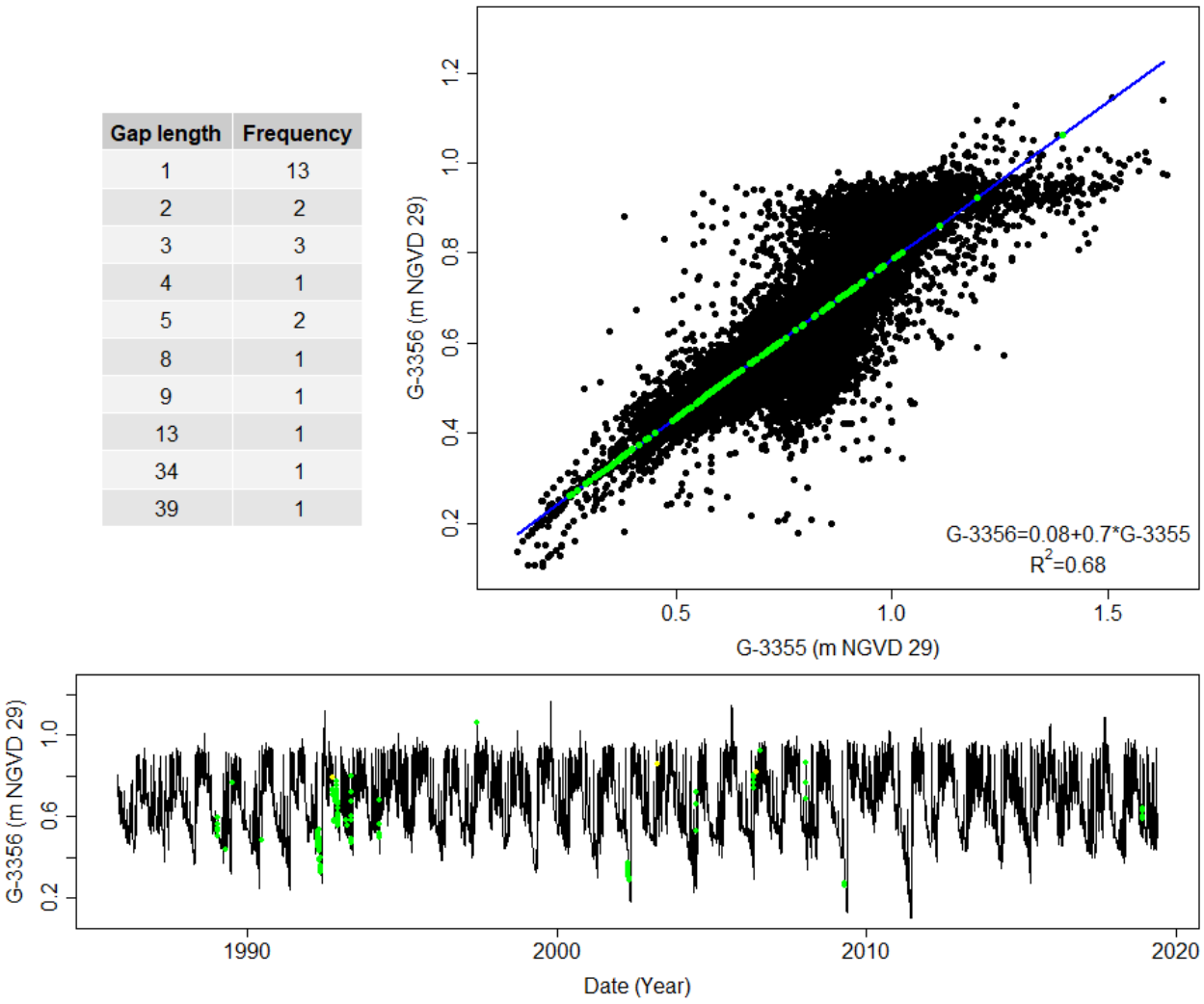

Figure S3: Record at well G-3356 – groundwater level at case study site S20 - is imputed using readings from Well G-3355. See caption to Figure S2 for more explanation regarding the subfigures.

Gap length	Frequency
1	7
2	9
3	7
4	3
5	2
6	1
7	1
9	1
13	2
14	1
36	1

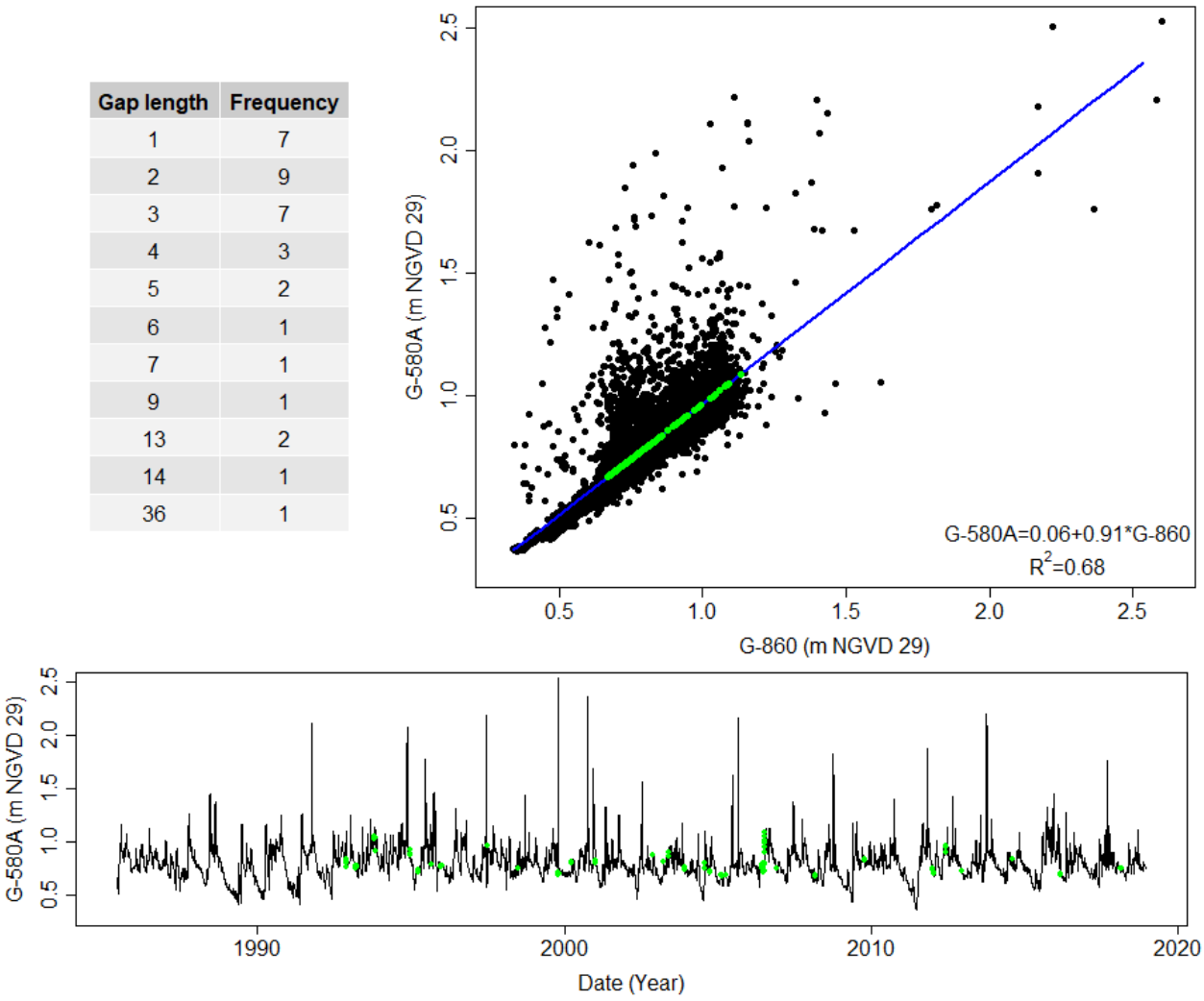

Figure S4: The record at G-580A – groundwater level at case study site S22 - is imputed using readings from well G-860. See caption to Figure S2 for more explanation regarding the subfigures.

Gap length	Frequency
1	7
2	4
3	2
5	1

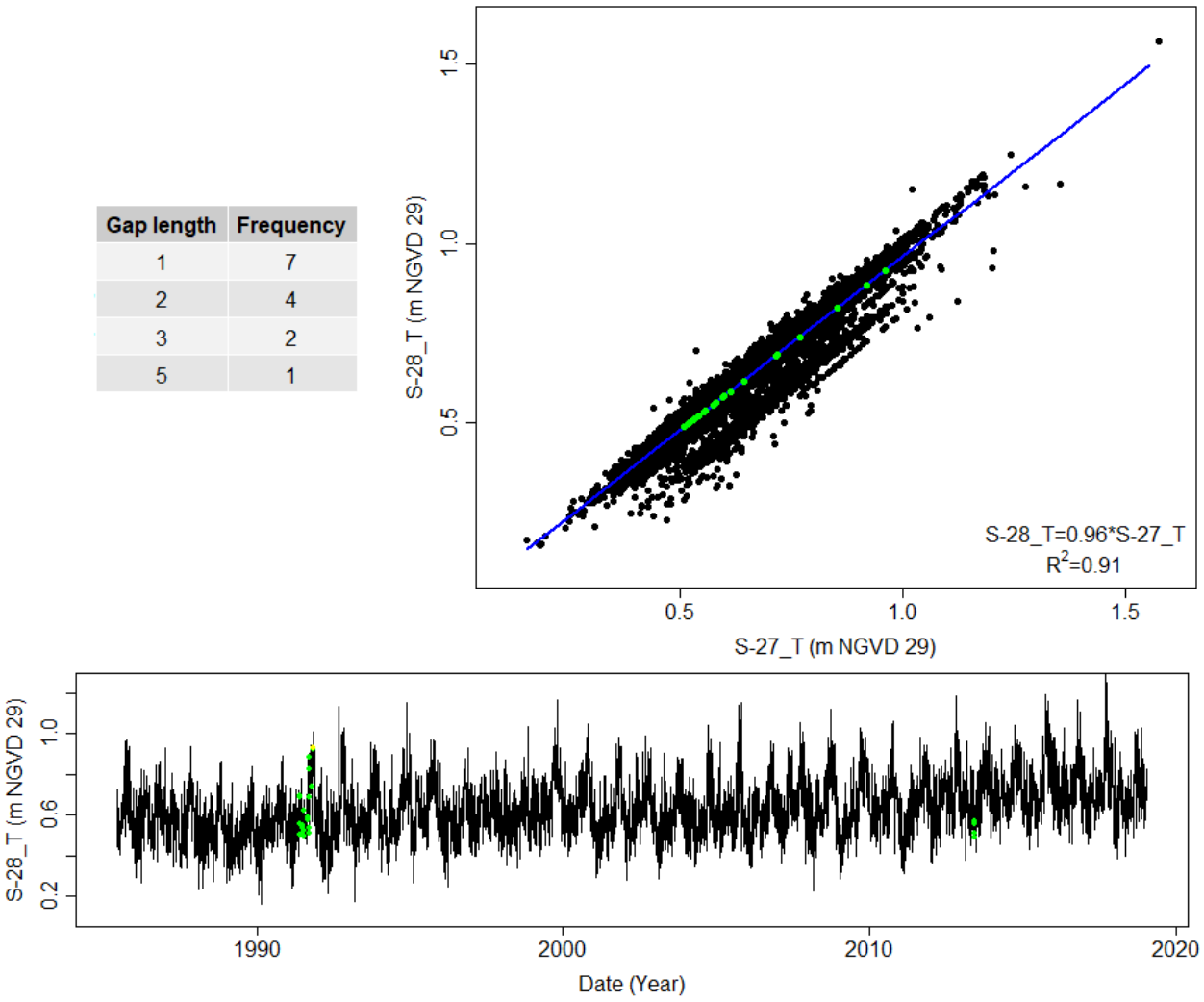

Figure S5: The record at S-28_T - O-sWL at case study site S28 - is imputed using readings from station S-27_T. See caption to Figure S2 for more explanation regarding the subfigures.

Gap length	Frequency
1	5
2	6
3	2
4	2
5	5
6	2
7	4
15	1
22	1
28	1
62	1
77	1

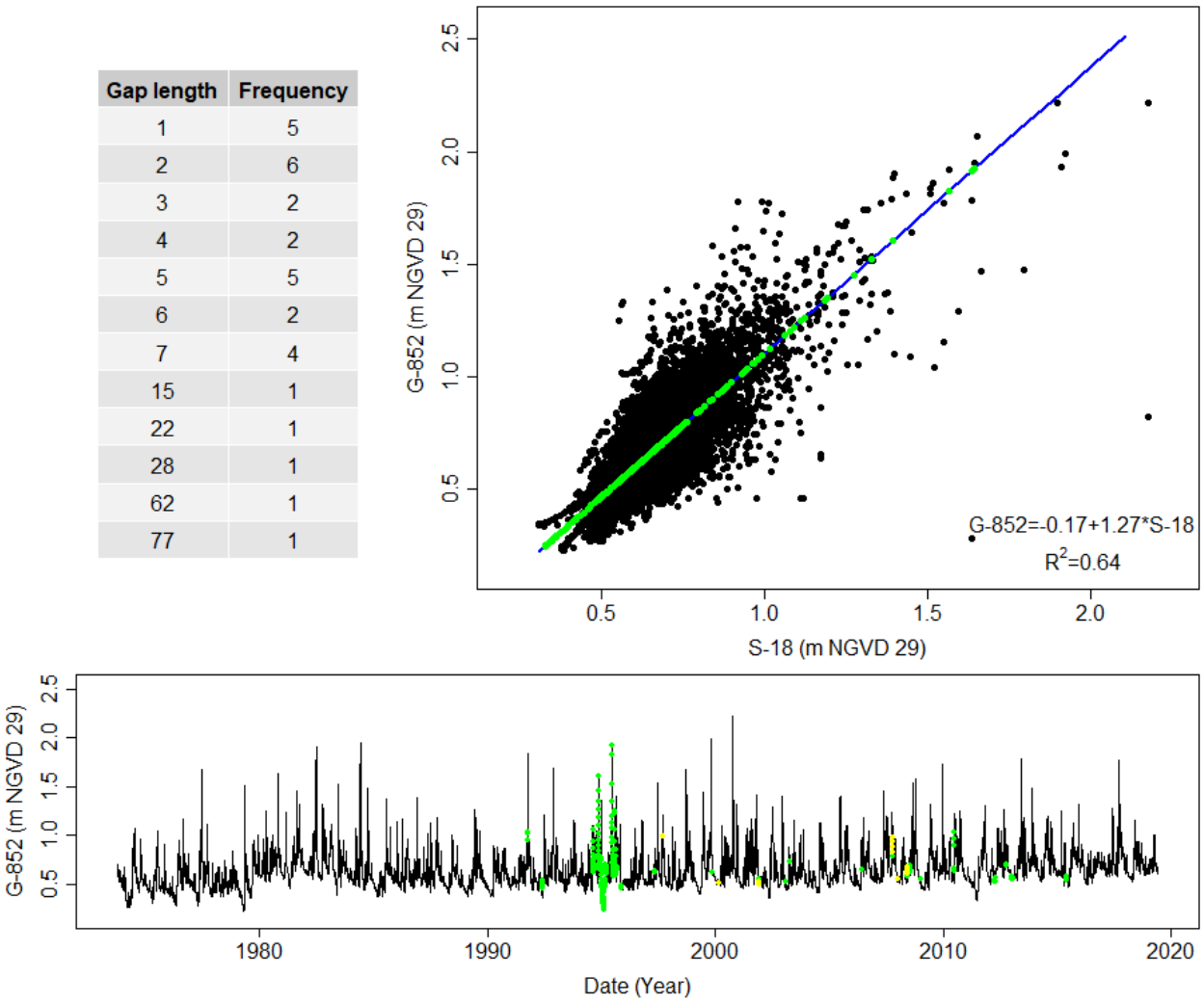

Figure S6: The record at G-852 – groundwater level at case study site S28 - is imputed using readings from well S-18. See caption to Figure S2 for more explanation regarding the subfigures.

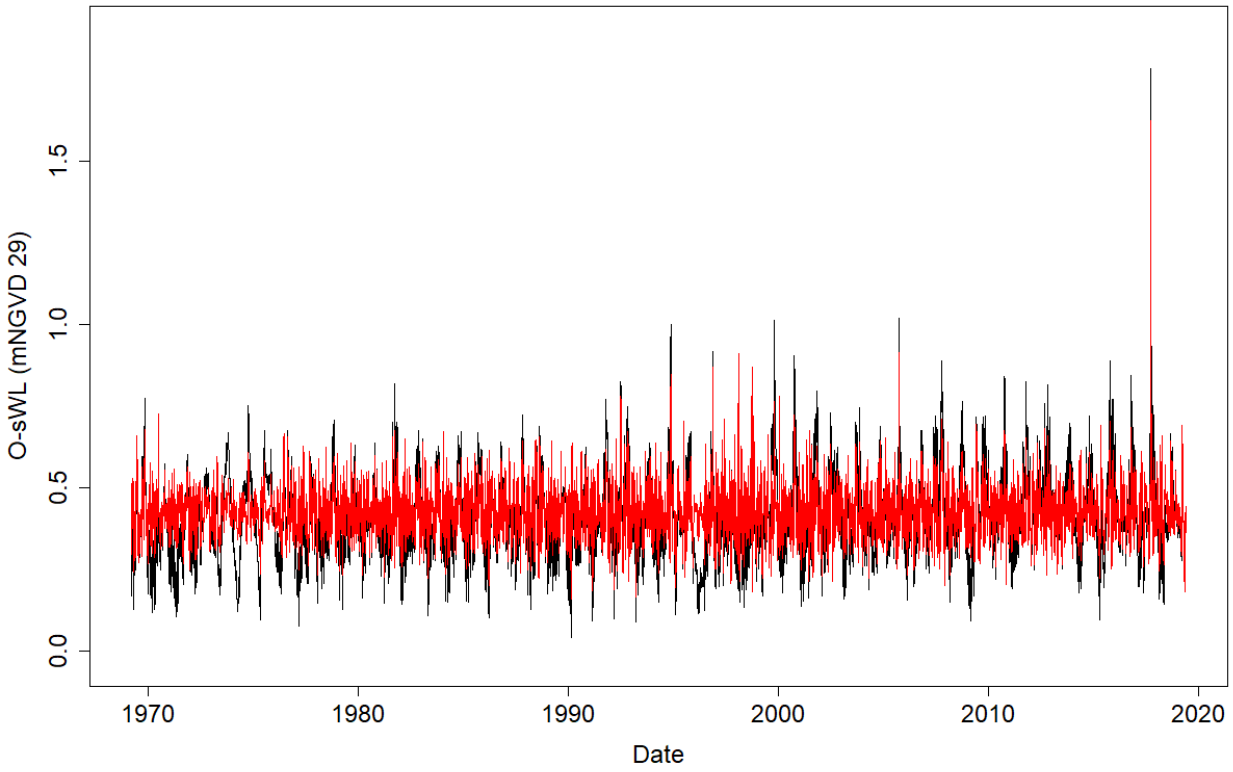

Figure S7: Measured (black lines) and detrended (red lines) O-sWL record at station S-20_T (site S20).

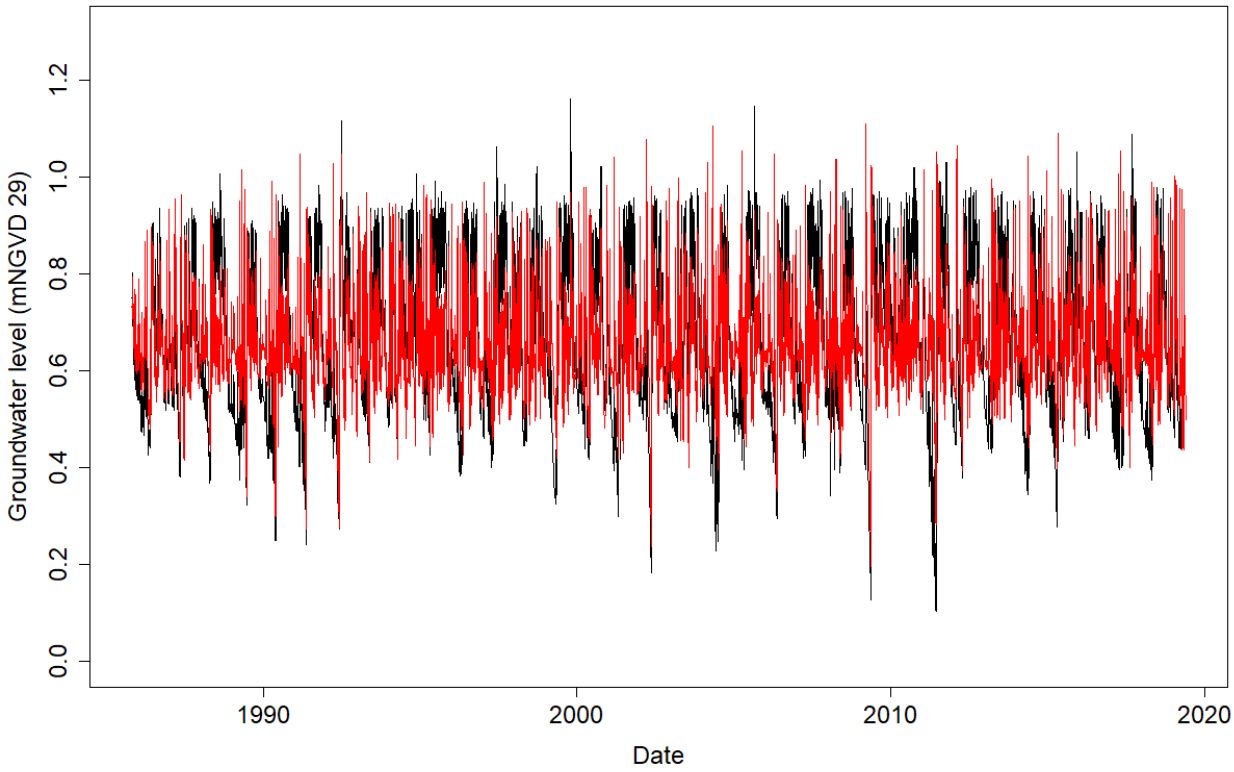

Figure S8: Measured (black lines) and detrended (red lines) record at Well G-3356 (site S20).

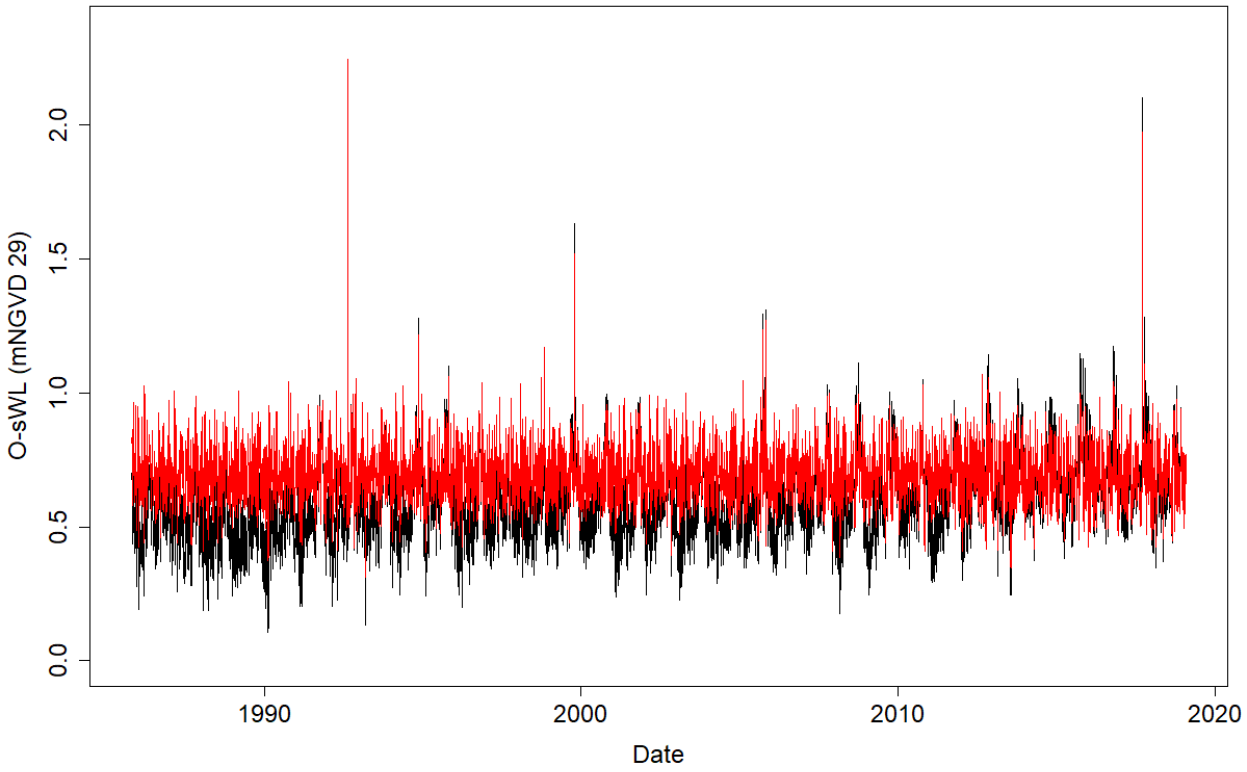

Figure S9: Measured (black lines) and detrended (red lines) O-sWL record at station S-22_T (site S22).

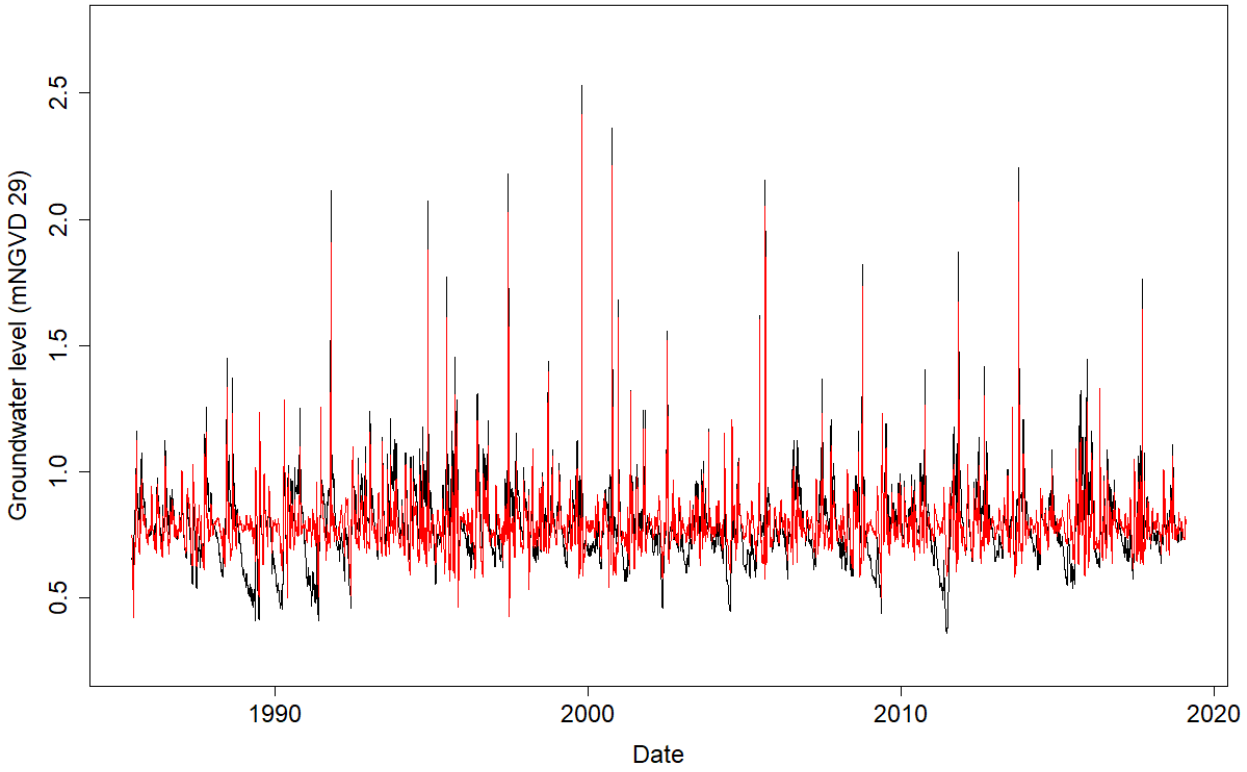

Figure S10: Measured (black lines) and detrended (red lines) record at Well G-580A (site S22).

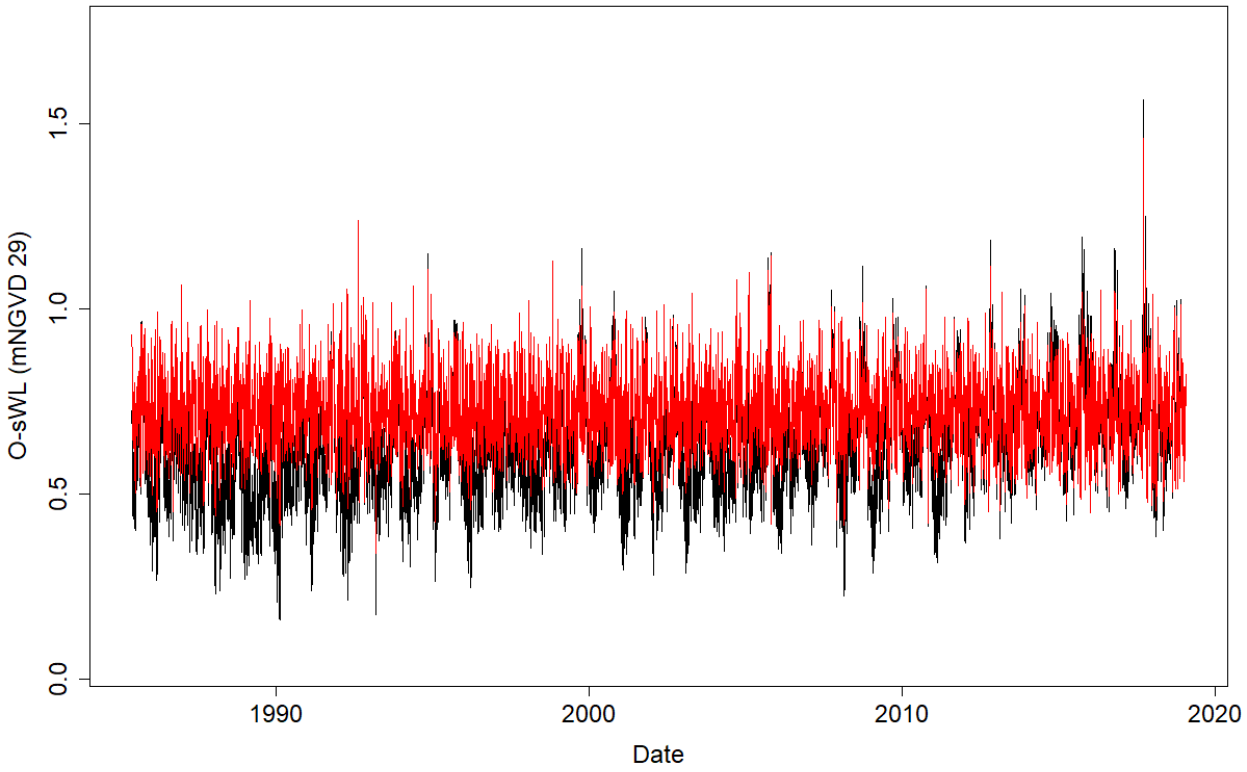

Figure S11: Measured (black lines) and detrended (red lines) O-sWL record at station S28_T (site S28).

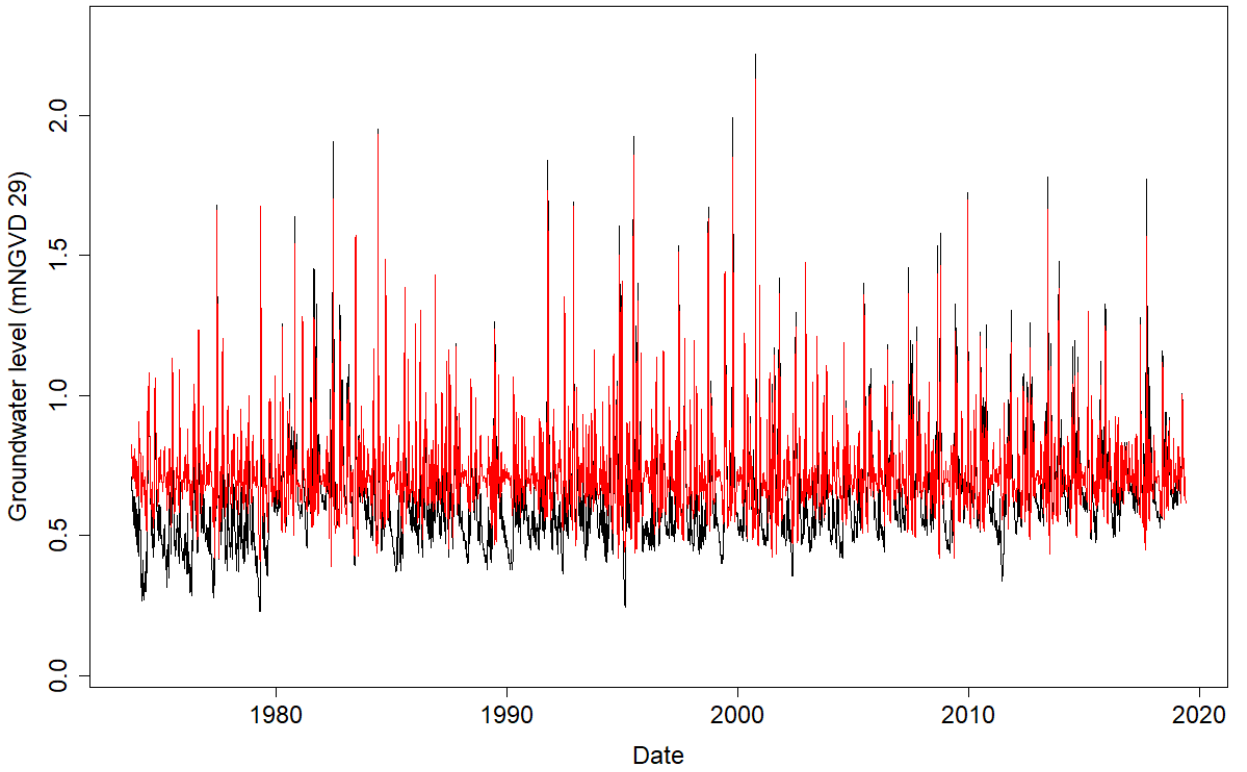

Figure S12: Measured (black lines) and detrended (red lines) record at Well G-852 (site S28).

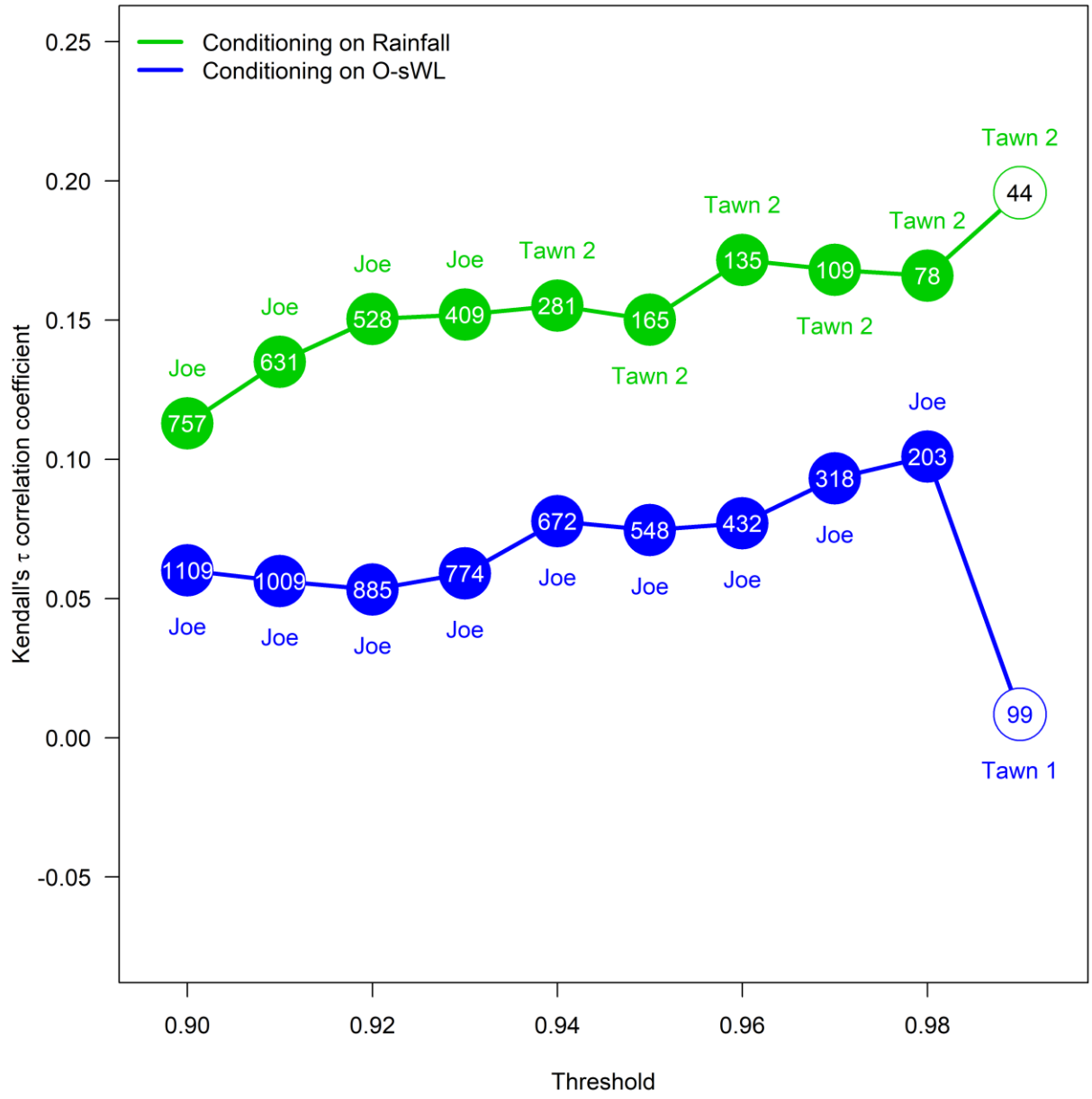

Figure S13: Kendall's τ correlation coefficient between rainfall and O-sWL for the sample conditioning on rainfall (green circles) and O-sWL (blue circles), given the threshold selected for the conditioning variable. The threshold is given as a percentile of the declustered data of the conditioning variable. Filled circles indicate strong evidence against H_0: $\tau = 0$. Numbers inside the circles denote the sample size while the name of the best fitting of 40 tested copulas (plus the independence copula) at a given threshold is printed above/below the associated circle. The results displayed in this Figure correspond to Site S20.

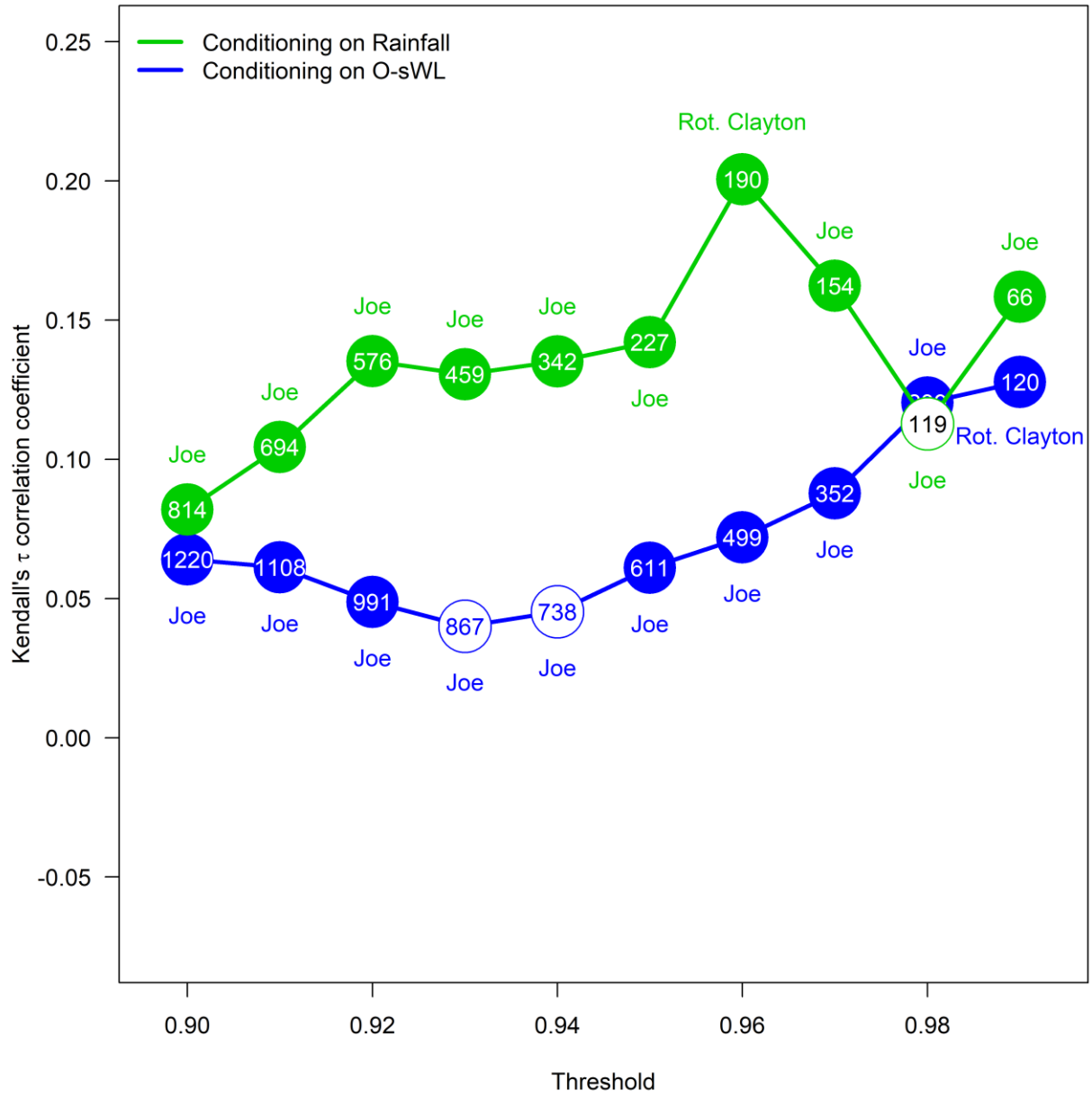

Figure S14: Sensitivity of the best fitting copula to threshold at Site S22. See caption to Figure S13 for additional explanation.

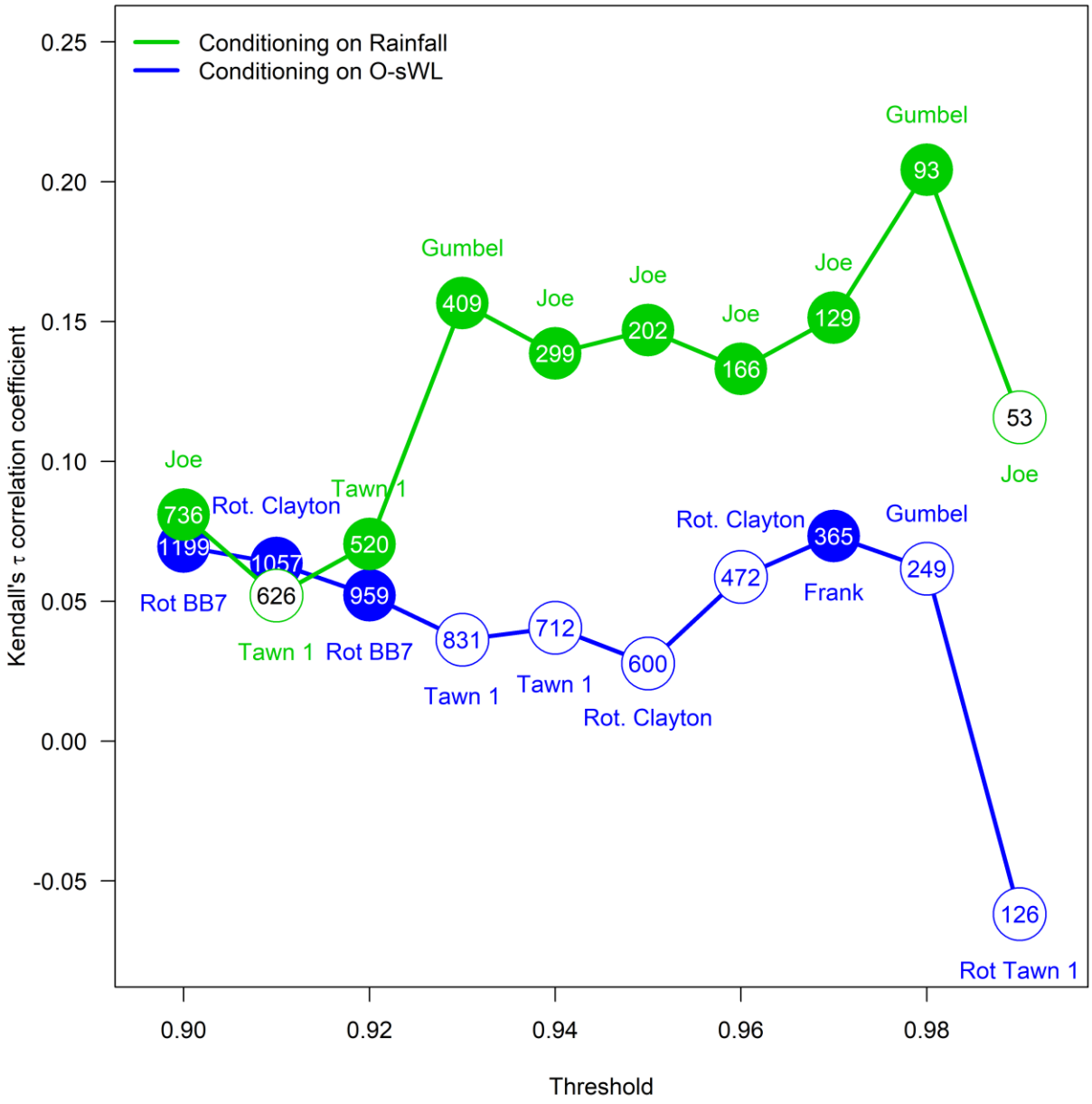

Figure S15: Sensitivity of the best fitting copula to threshold at Site S28. See caption to Figure S13 for additional explanation.

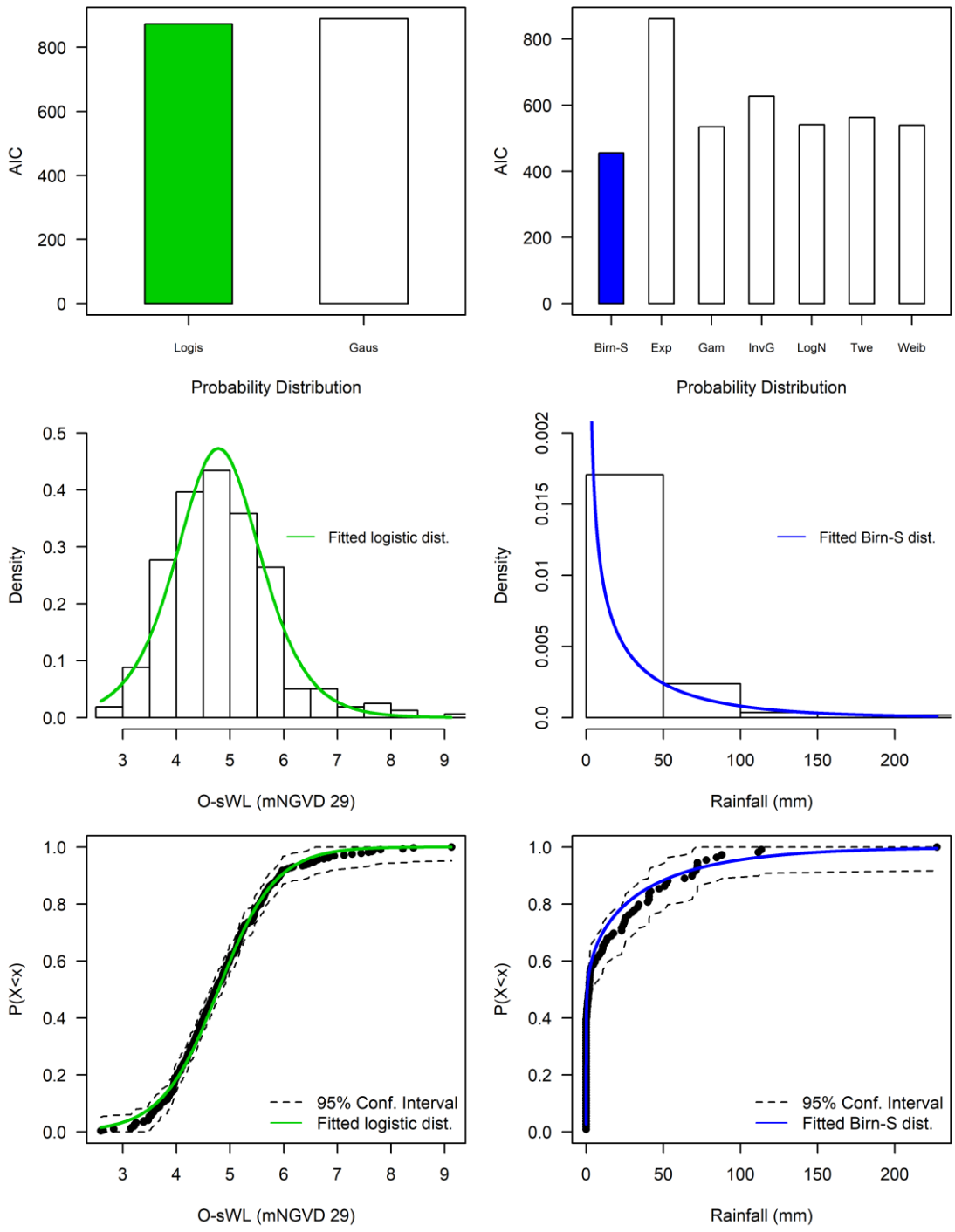

Figure S16: Goodness-of-fit of parametric distributions fitted to on-conditioning variables. Left(right)-hand columns show fits to O-sWL(rainfall) in the samples where rainfall(O-sWL) is the conditioning variable. Top row: AIC for Logistic (Logis) and Gaussian (Gaus) distributions fitted to rainfall and Birnbaum-Saunders (Birn-S), Exponential (Exp), Gamma (Gam), Inverse Gaussian (InvG), Lognormal (LogN), Tweedie (Twe) and Weibull (Weib) fitted to O-sWL. Coloured bar denotes AIC of selected distribution. Middle row: Probability density function of selected distribution superimposed onto histogram of observations. Bottom row: Empirical Cumulative Distribution Function (CDF) of the observations (dots) shown alongside the CDF of the selected distribution. Dashed lines denote 95% confidence interval of the empirical CDF constructed using the Dvoretzky–Kiefer–Wolfowitz inequality. Results for Site S20 above.

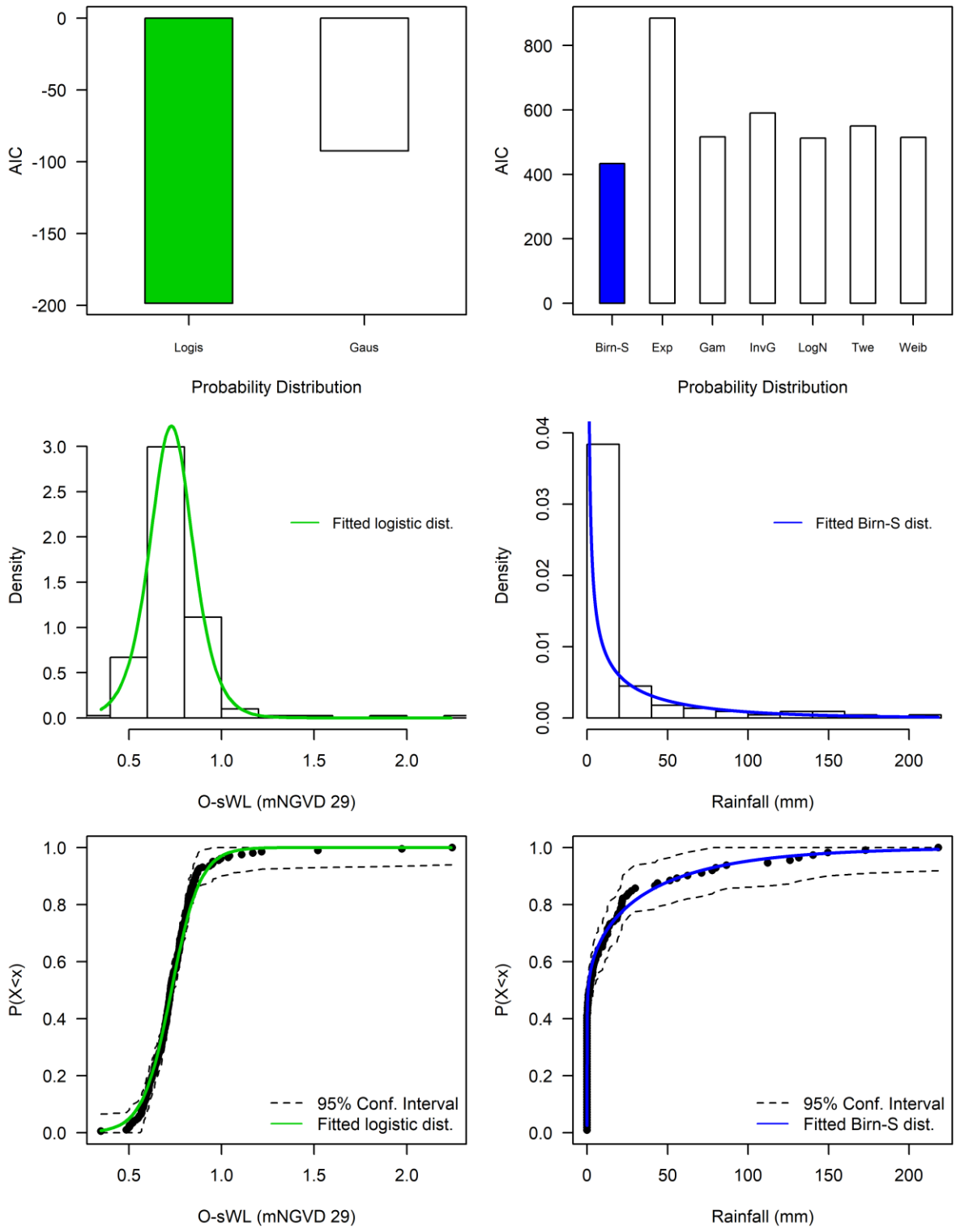

Figure S17: Goodness-of-fit of the parametric distributions fitted to the non-conditioning variables in the 2D analysis at site S22. See caption to Figure S16 for additional explanation.

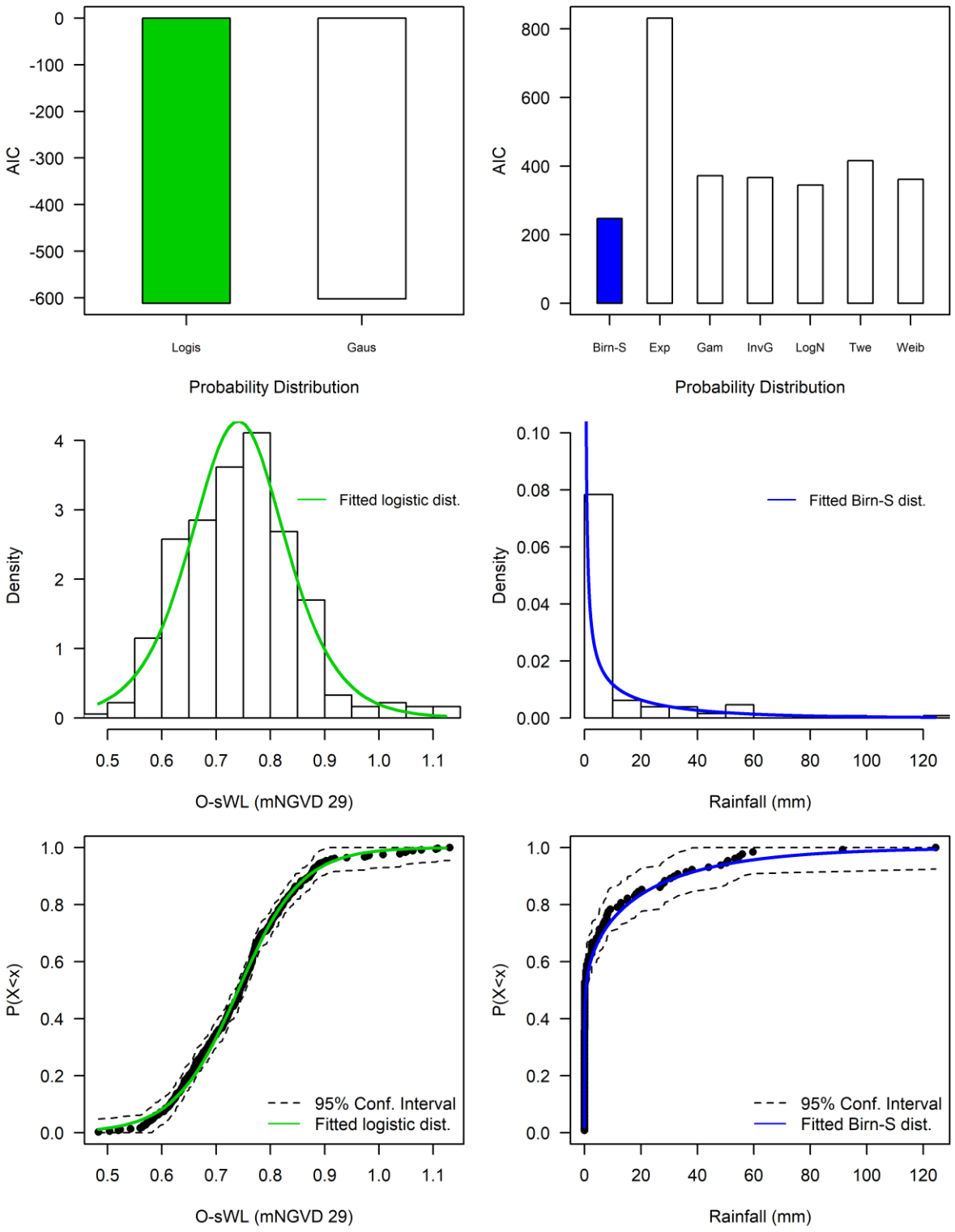

Figure S18: Goodness-of-fit of the parametric distributions fitted to the non-conditioning variables in the 2D analysis at site S28. See caption to Figure S16 for additional explanation.

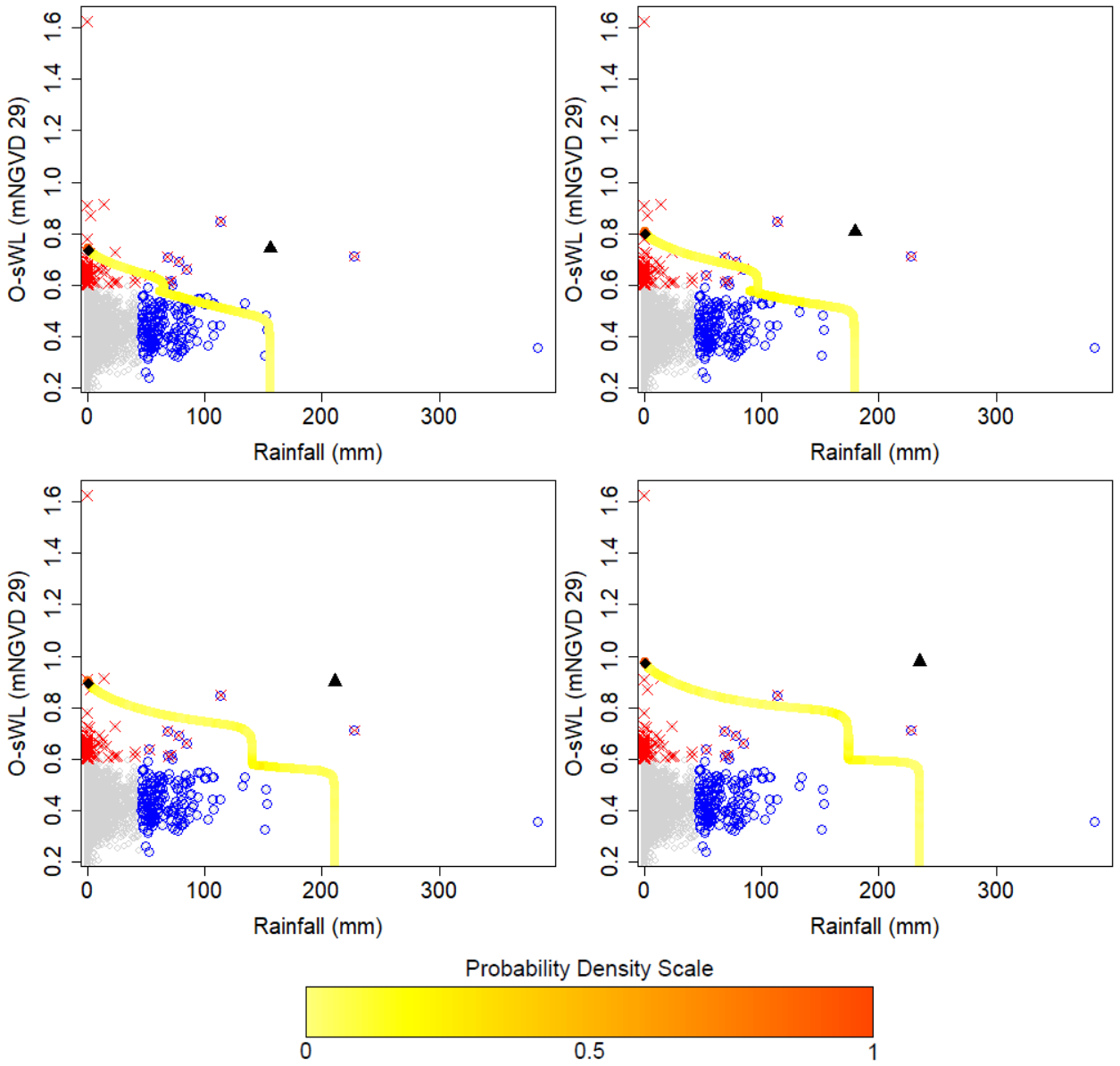

Figure S19: Comparison of the design events at site S20 obtained using the two-sided conditional sampling approach (diamonds) and the existing SFWMD approach (triangles) for return periods of (upper left) 10-, (upper right) 20-, (lower left) 50- and (lower right) 100-years. Quantile-isolines are superimposed onto plots of the observations, with blue circles (red crosses) denoting observations exceeding the rainfall(O-sWL) threshold and those exceeding neither threshold plotted in grey. Colored contours signify the relative likelihood of events along an isoline.

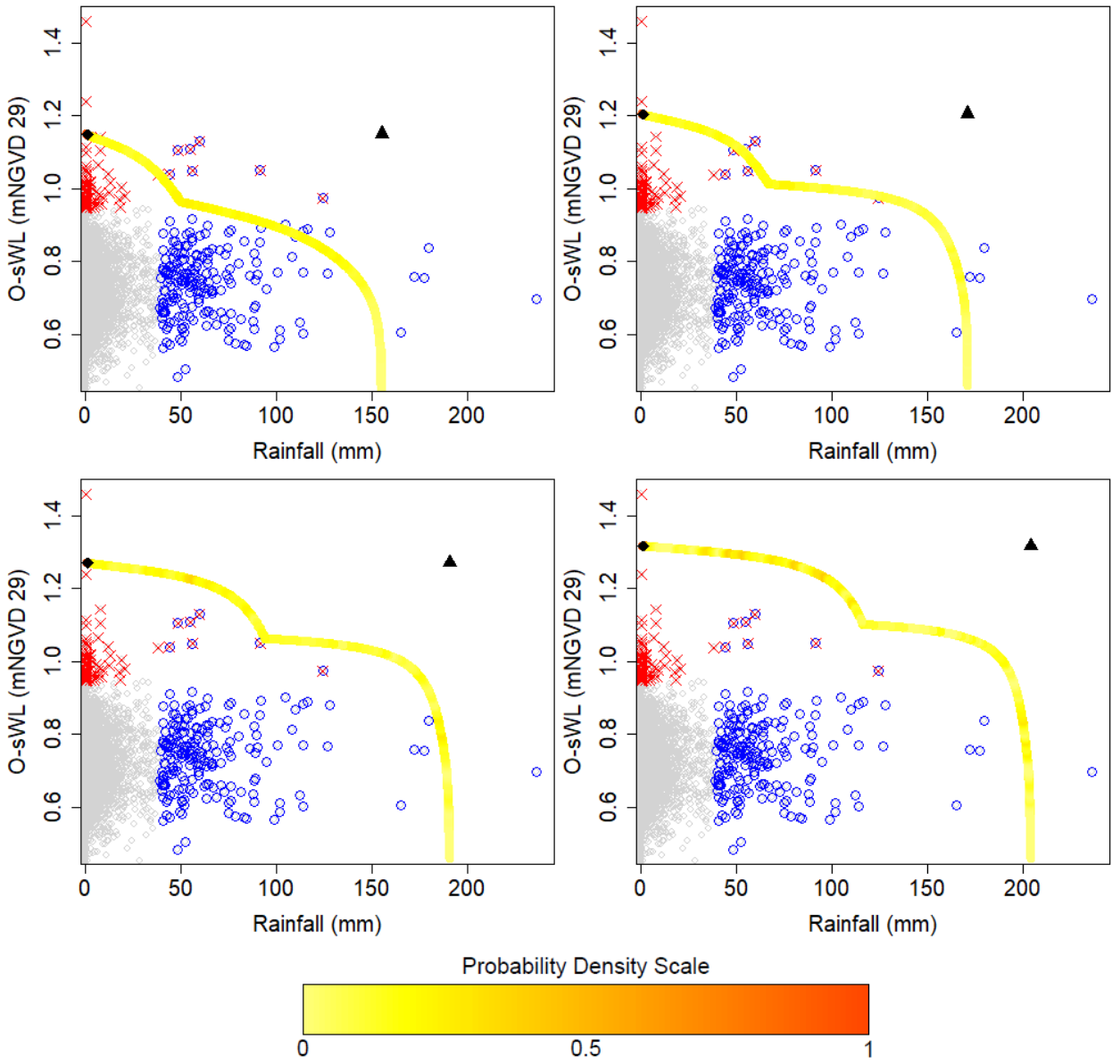

Figure S20: Comparison of the design events at site S28 obtained using the two-sided conditional sampling approach (diamonds) and the existing SFWMD approach (triangles) for return periods of (upper left) 10-, (upper right) 20-, (lower left) 50- and (lower right) 100-years. For additional explanation see caption to Figure S19.

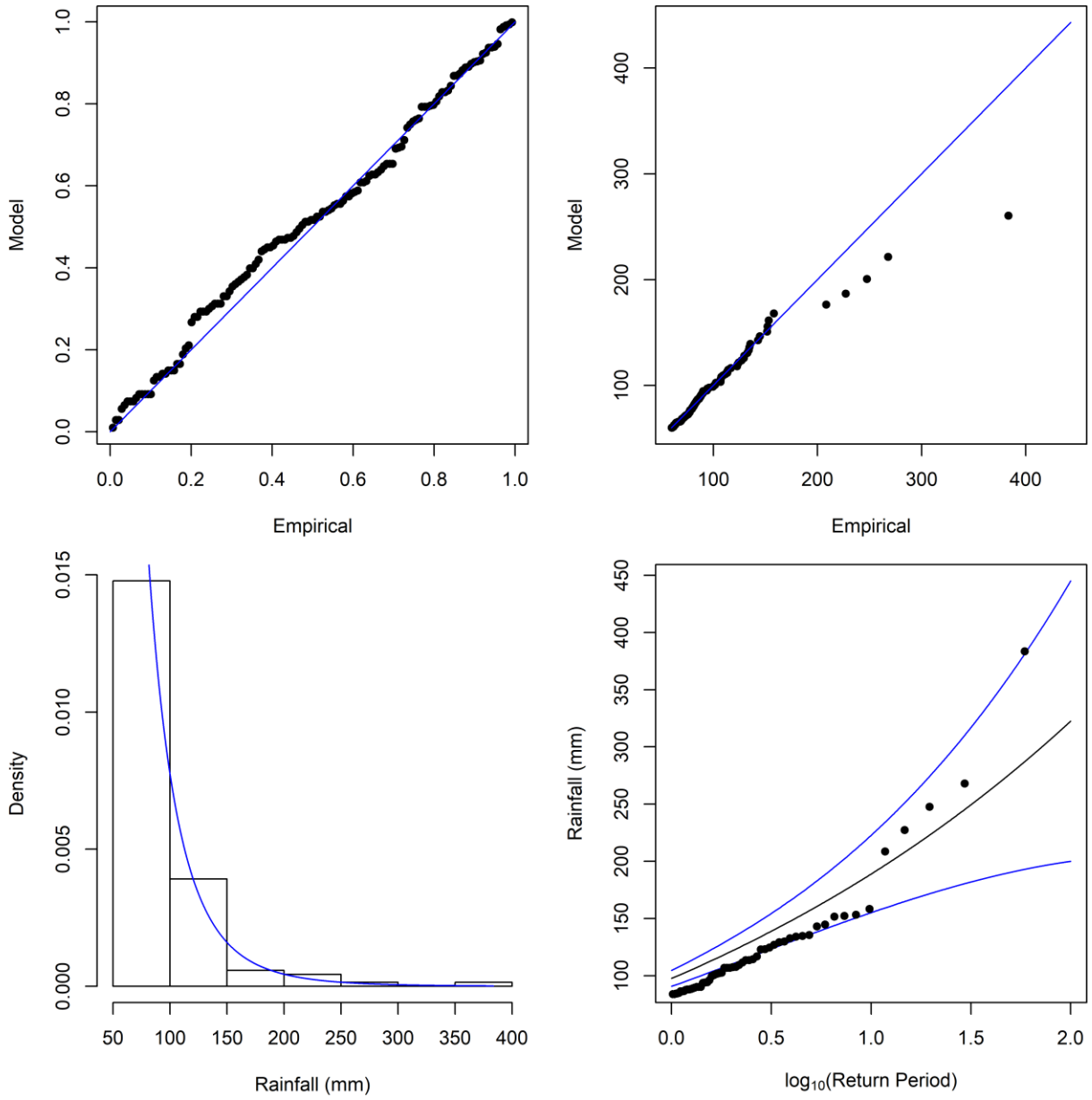

Figure S21: Diagnostic plots for assessing the goodness-of-fit of the Generalized Pareto Distribution (GPD) to the declustered rainfall, O-sWL and groundwater level records. Upper left: Probability-Probability (P-P) plot. Cumulative distribution function of the model, in this case the GPD, plotted against the empirical CDF at the observed points. Points lying along y=x (blue line) indicate a good fit while notable deviations from the line are evidence against the observations being realizations from a GPD. Upper right: Quantile-Quantile (Q-Q) plot. Theoretical quantiles of the model, in this case the GPD, plotted against the corresponding (empirical) quantiles calculated from the observations. Points lying along y=x (blue line) indicate a good fit while notable deviations from the line are evidence against the observations being realizations from a GPD. Lower left: Probability density function of the fitted GPD (blue line) superimposed onto a histogram of the observations. Lower right: Empirically estimated return periods (points) plotted alongside the return periods assigned by the fitted GPD (black line). The 95% confidence interval for the GPD estimates are also provided (blue lines). Rainfall at Site S20 shown above.

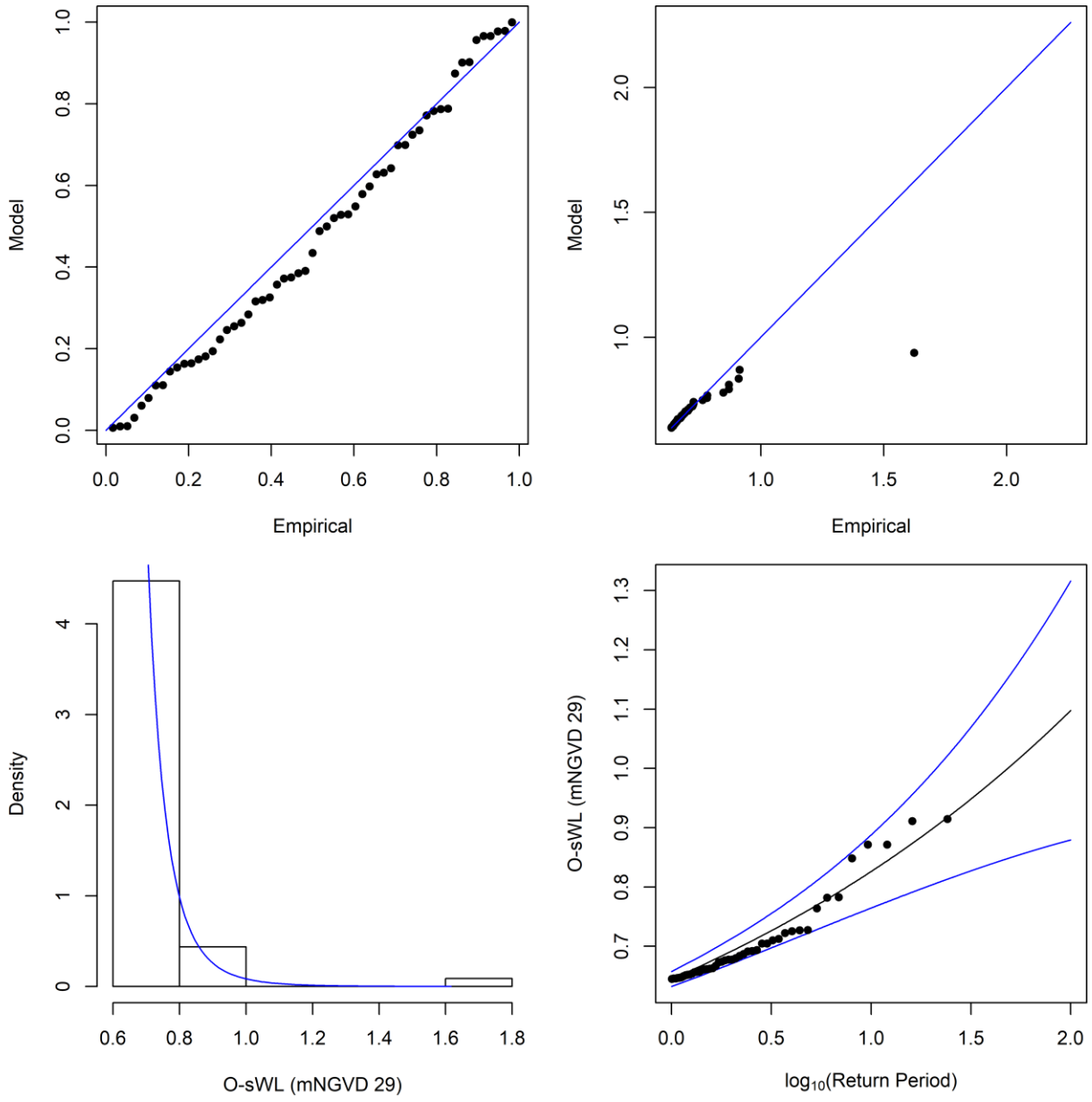

Figure S22: Diagnostic plots for assessing the goodness-of-fit of the GPD to the declustered O-sWL record at site S20. See caption to Figure S21 for additional explanation.

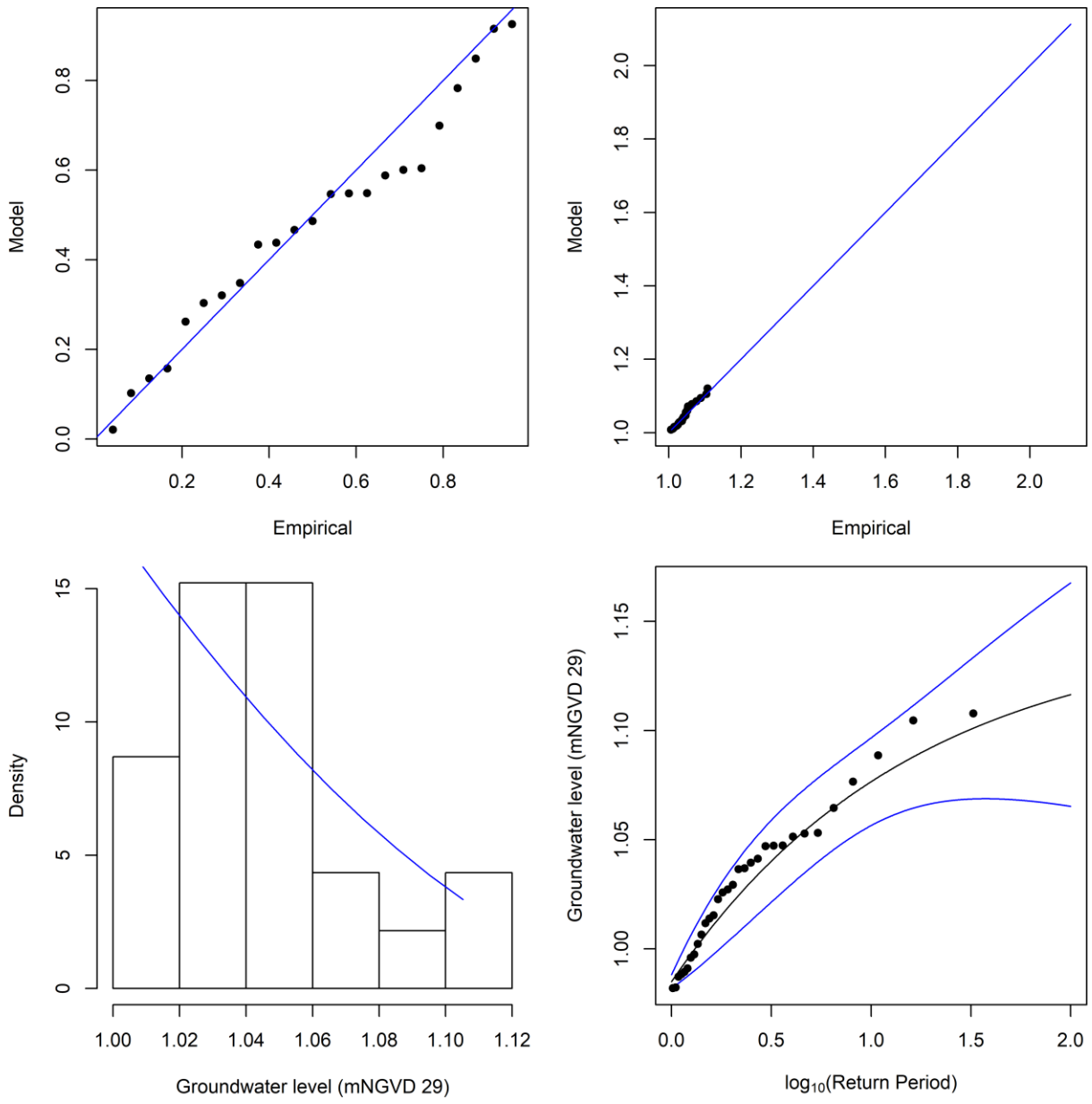

Figure S23: Diagnostic plots for assessing the goodness-of-fit of the GPD to the declustered groundwater level record at site S20. See caption to Figure S21 for additional explanation.

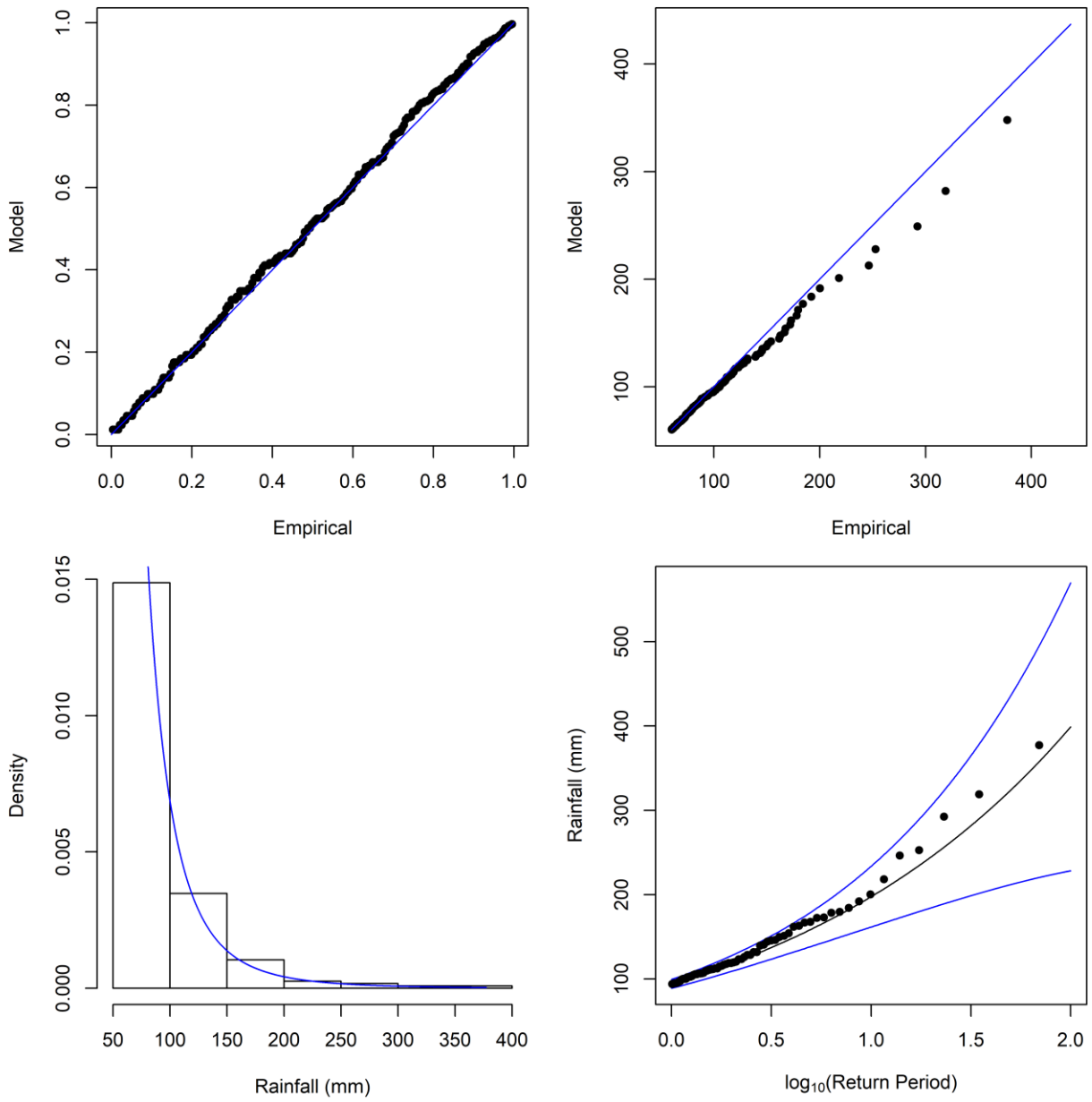

Figure S24: Diagnostic plots for assessing the goodness-of-fit of the GPD to the declustered rainfall record at site S22. See caption to Figure S21 for additional explanation.

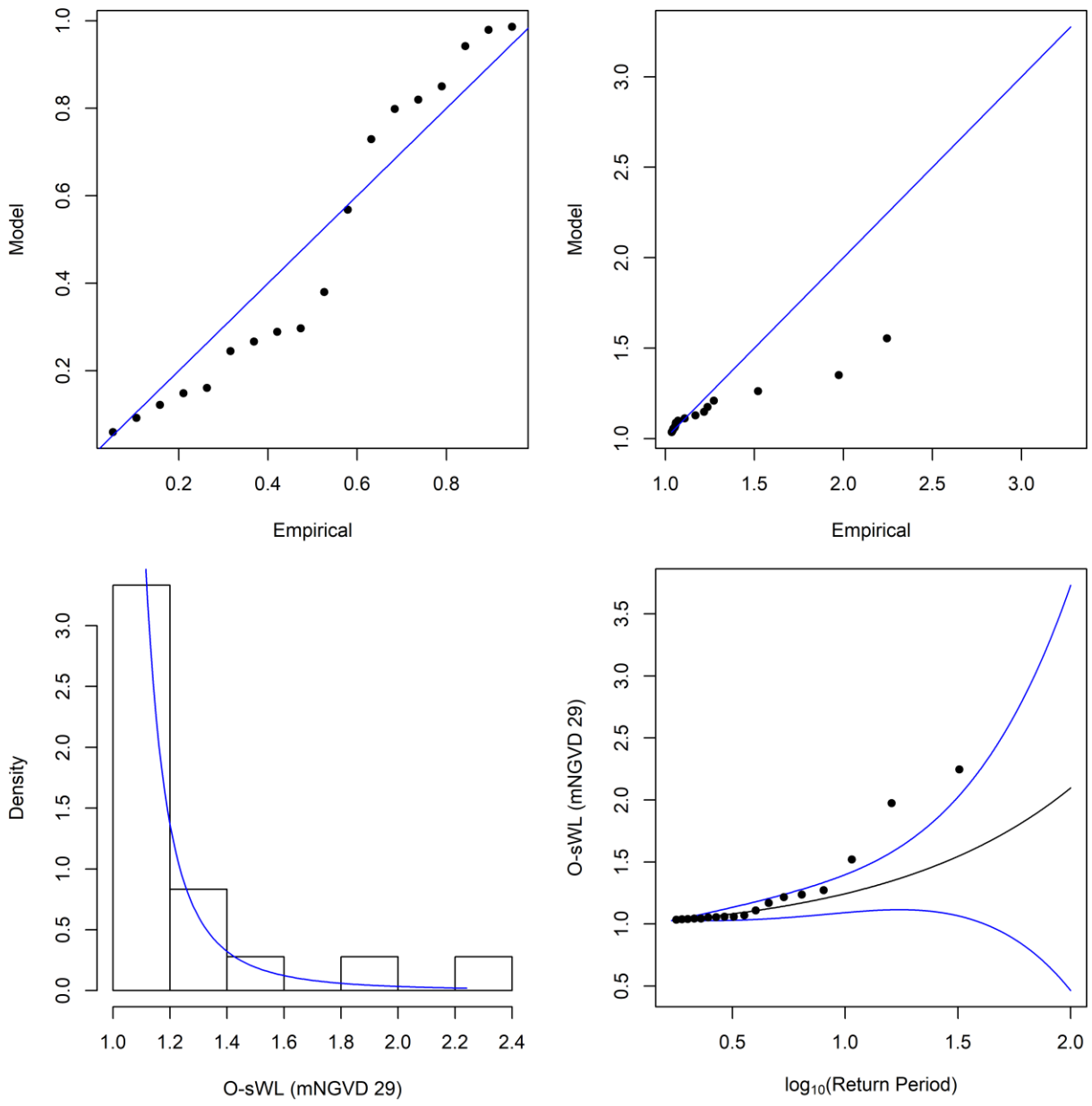

Figure S25: Diagnostic plots for assessing the goodness-of-fit of the GPD to the declustered O-sWL record at site S22. See caption to Figure S21 for additional explanation.

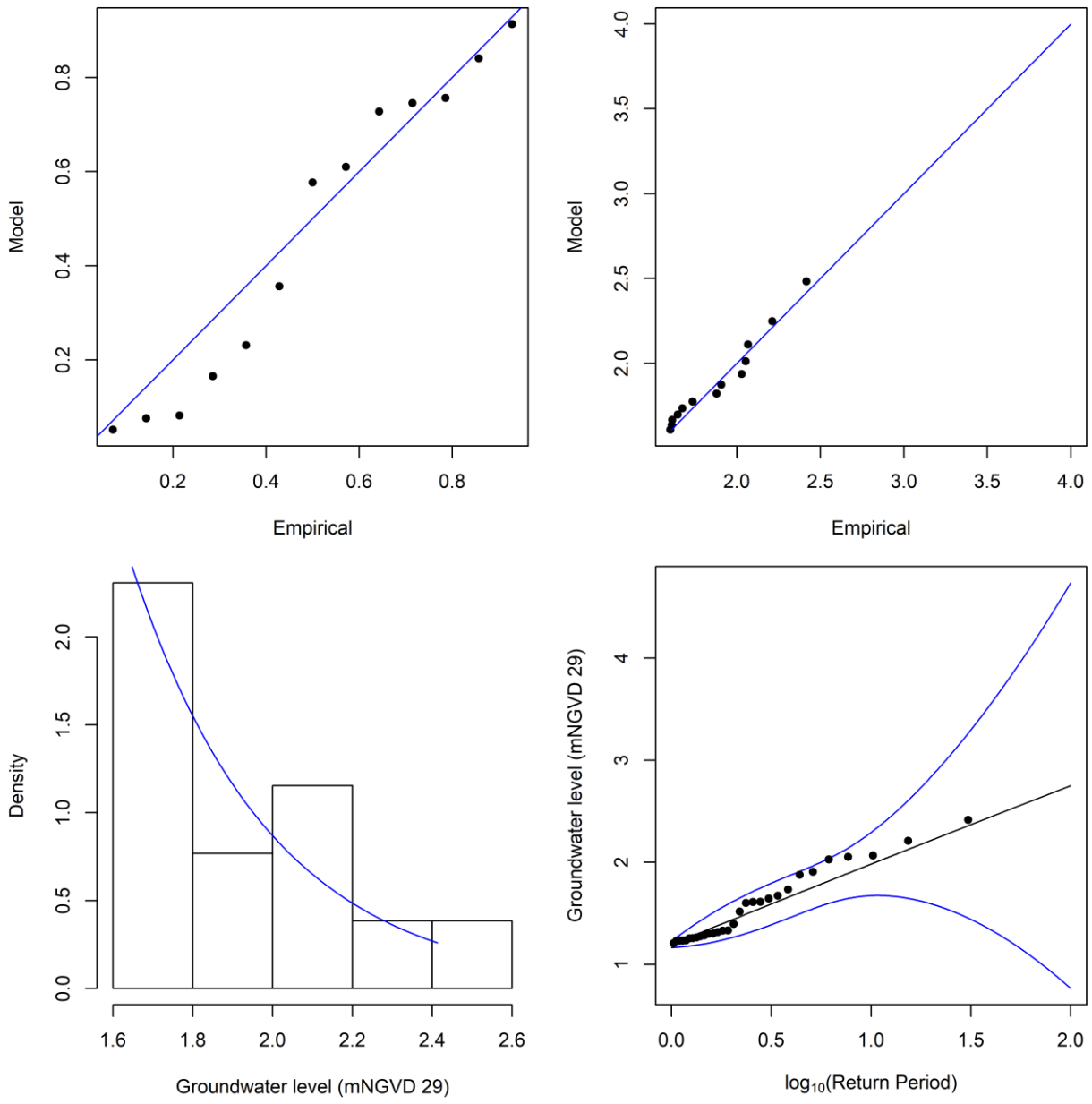

Figure S26: Diagnostic plots for assessing the goodness-of-fit of the GPD to the declustered groundwater level record at site S22. See caption to Figure S21 for additional explanation.

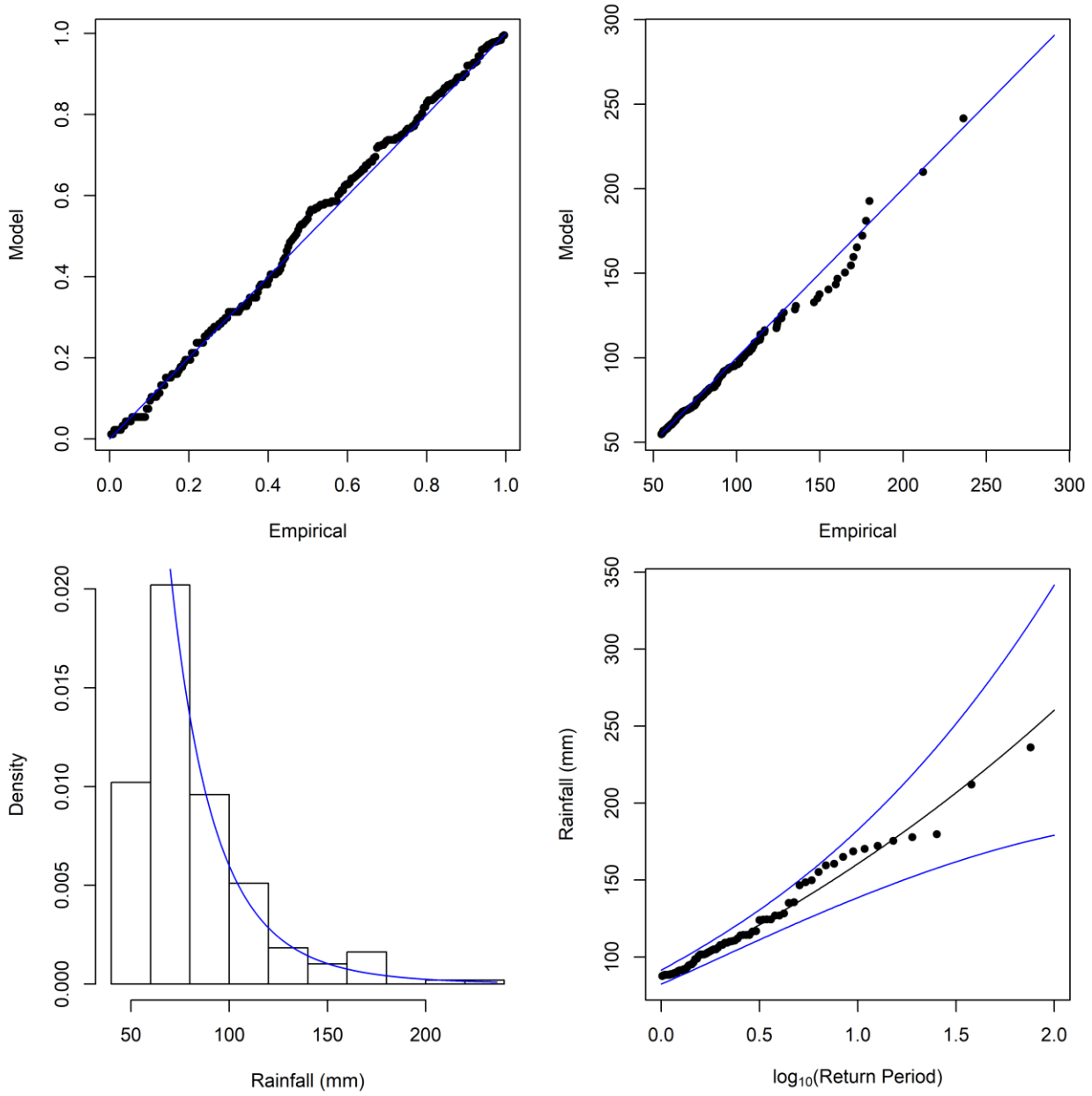

Figure S27: Diagnostic plots for assessing the goodness-of-fit of the GPD to the declustered rainfall record at site S28. See caption to Figure S21 for additional explanation.

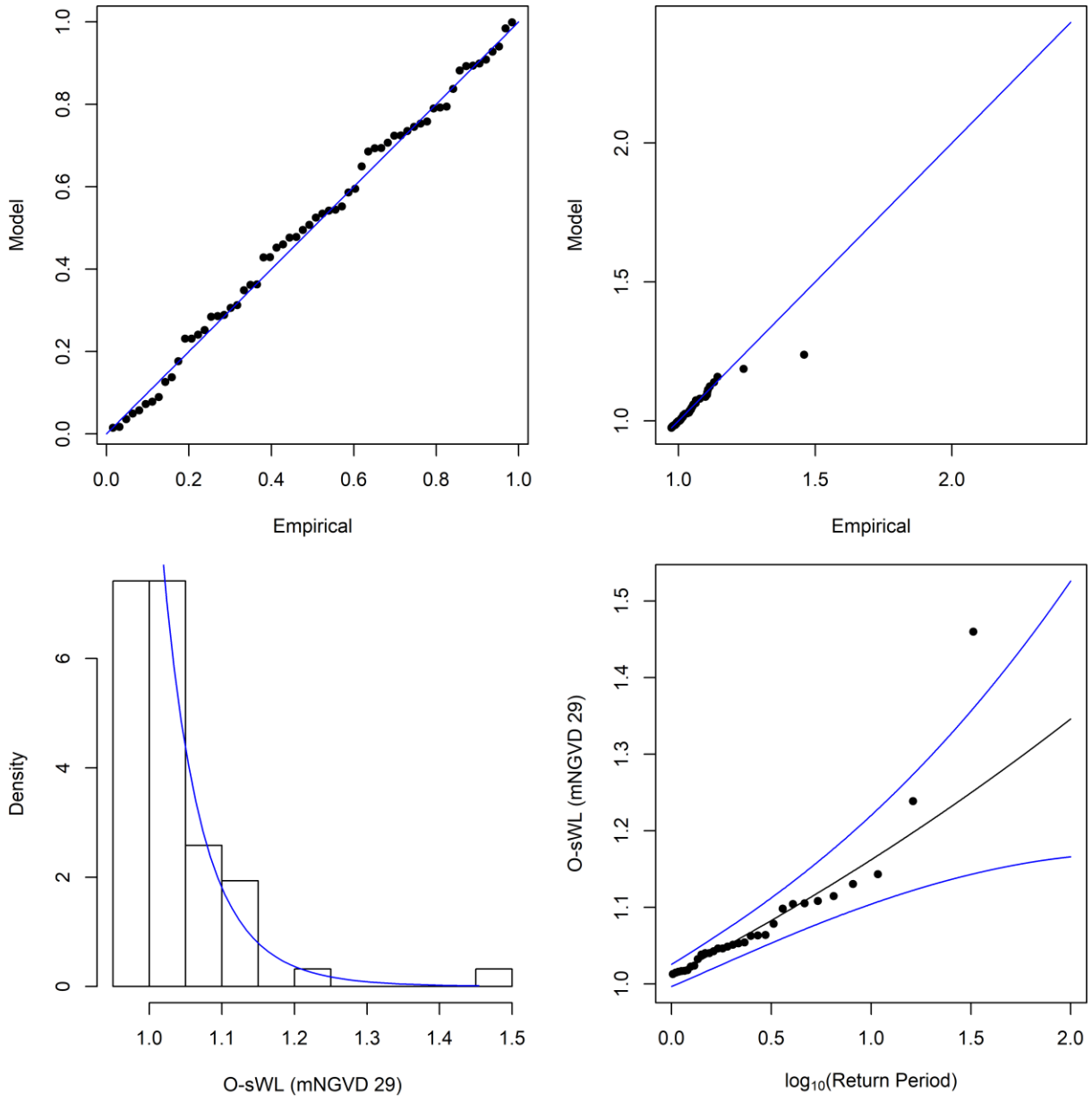

Figure S28: Diagnostic plots for assessing the goodness-of-fit of the GPD to the declustered O-sWL record at site S28. See caption to Figure S21 for additional explanation.

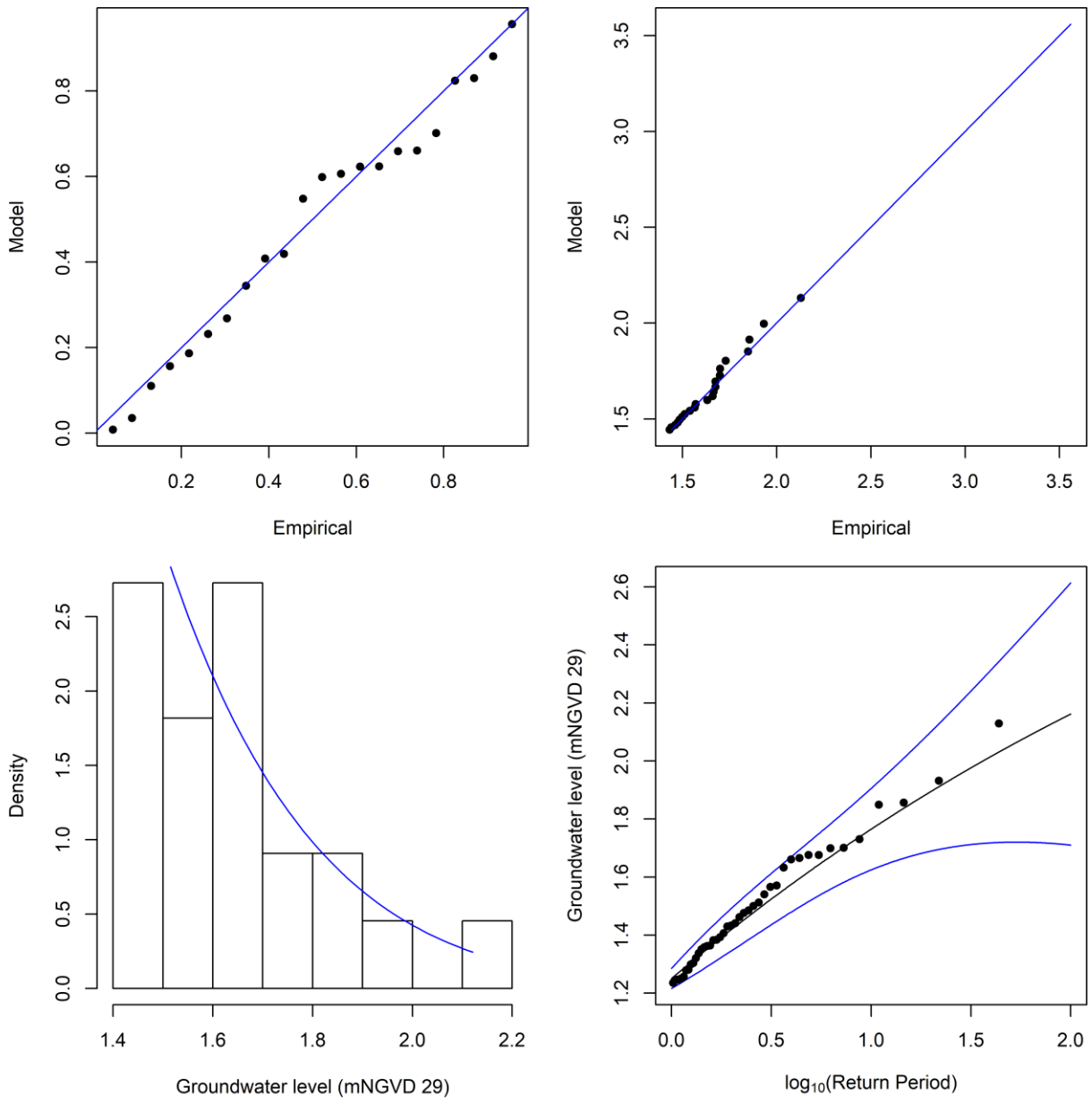

Figure S29: Diagnostic plots for assessing the goodness-of-fit of the GPD to the declustered groundwater level record at site S28. See caption to Figure S21 for additional explanation.

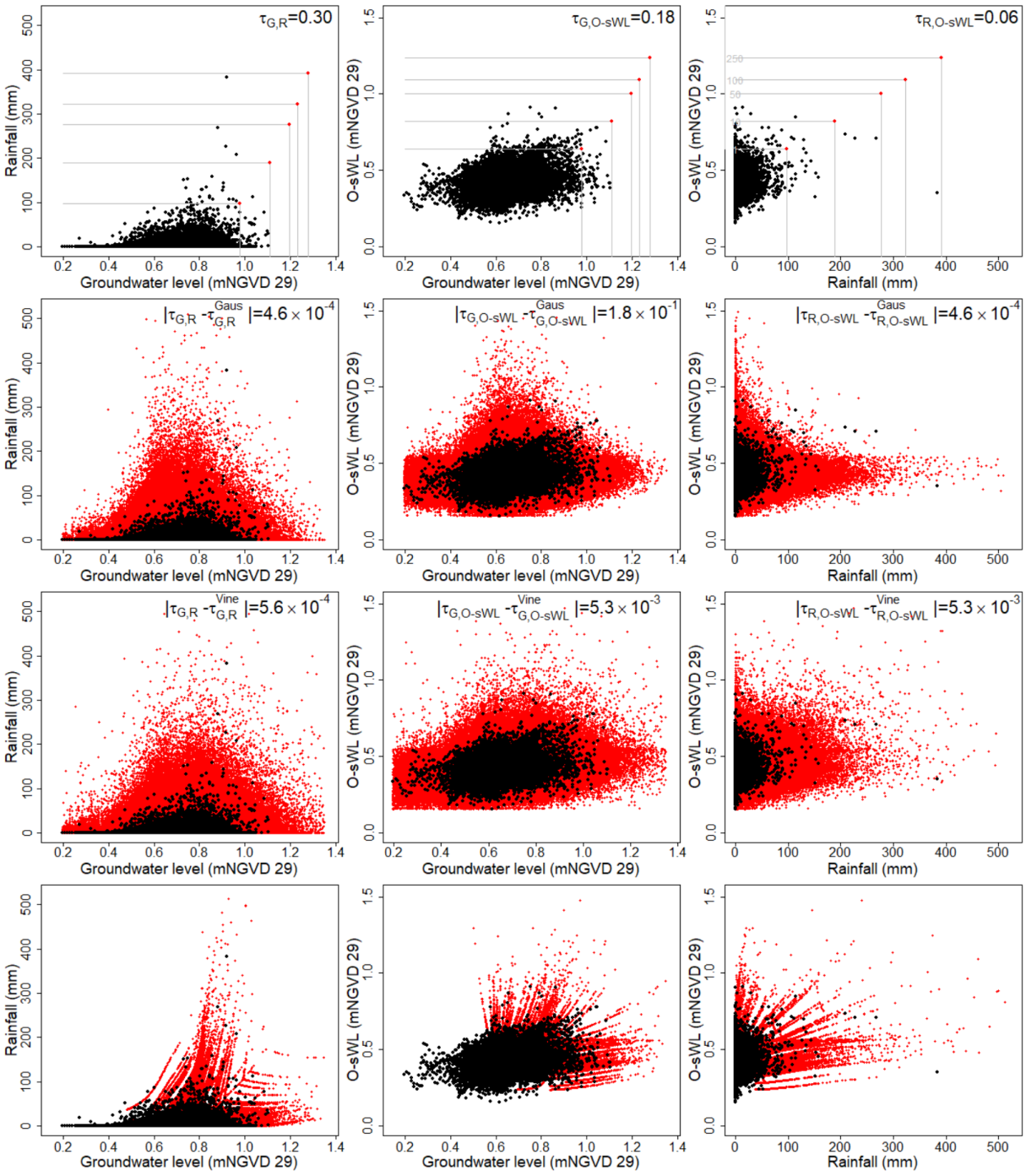

Figure S30: Goodness of fit of the 3D statistical models. 1st row: Pairwise plots of the observed data (black dots) shown alongside design events, under the assumption of full dependence (red dots). Kendall's τ coefficients calculated from the paired observations are given in the upper right-hand corner of each plot. 2nd row: Pair plots of the observed data (black dots) along with a sample from the fitted Gaussian copula, representative of 10,000 years, and transformed back to the original scale (red dots). Absolute difference in the Kendall's τ coefficients from the observations and Gaussian copula sample are given in the upper right-hand corner of each plot. 3rd row: As in the 2nd row but for the Vine copula model. 4th row: As in the 2nd row but for the HT04 model. Results are shown for site S20 above.

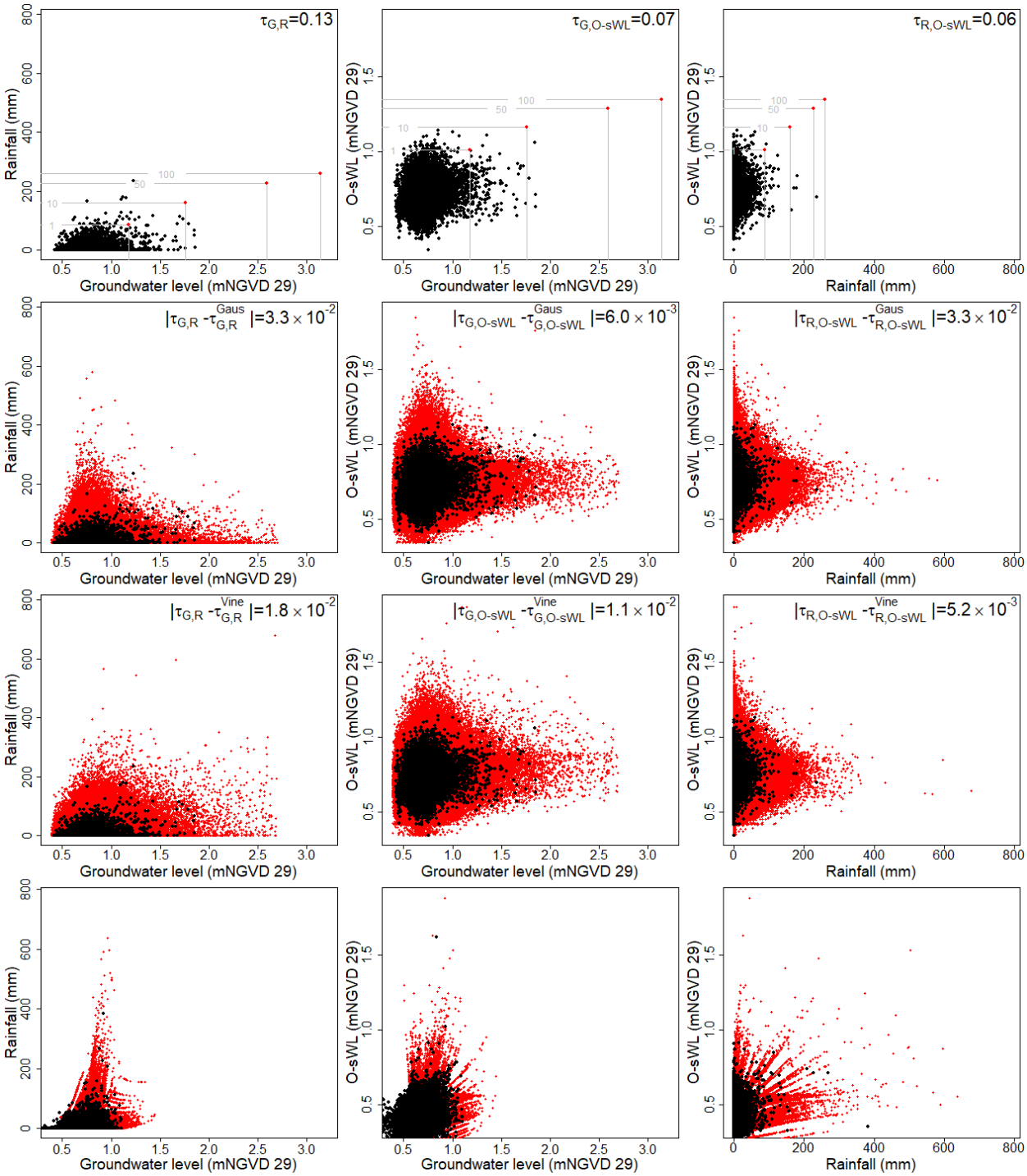

Figure S31: Goodness of fit of the 3D statistical models at site S28. See caption to Figure S29 for further explanation.

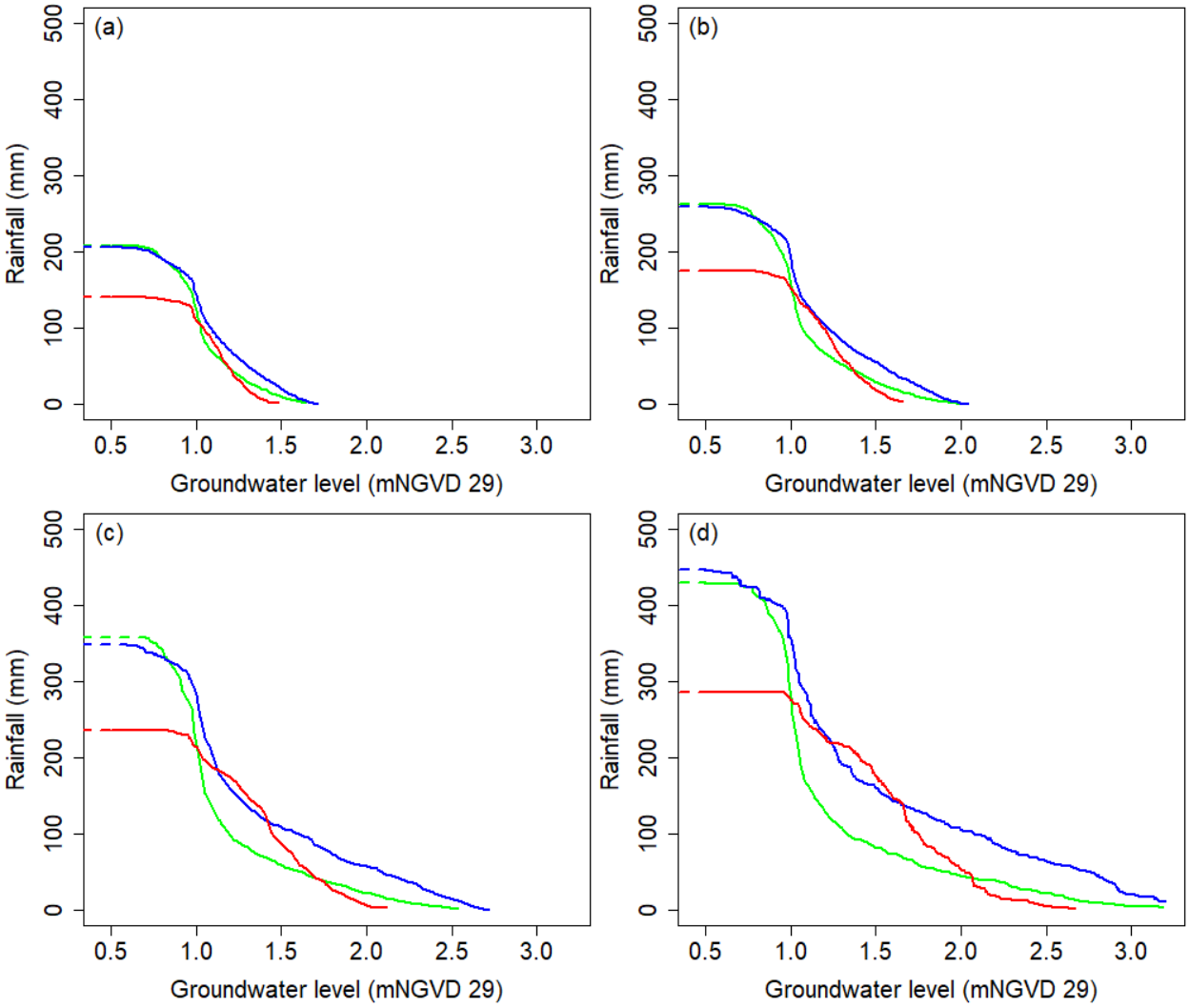

Figure S32: Isolines of rainfall and groundwater level at Site S22, obtained using the 10,000-year synthetic event records, from the Gaussian copula (blue), Vine copula (green) and HT04 model (red) for return periods of (a) 10-, (b) 20-, (c) 50- and (d) 100-years. Dotted lines represent extrapolation.

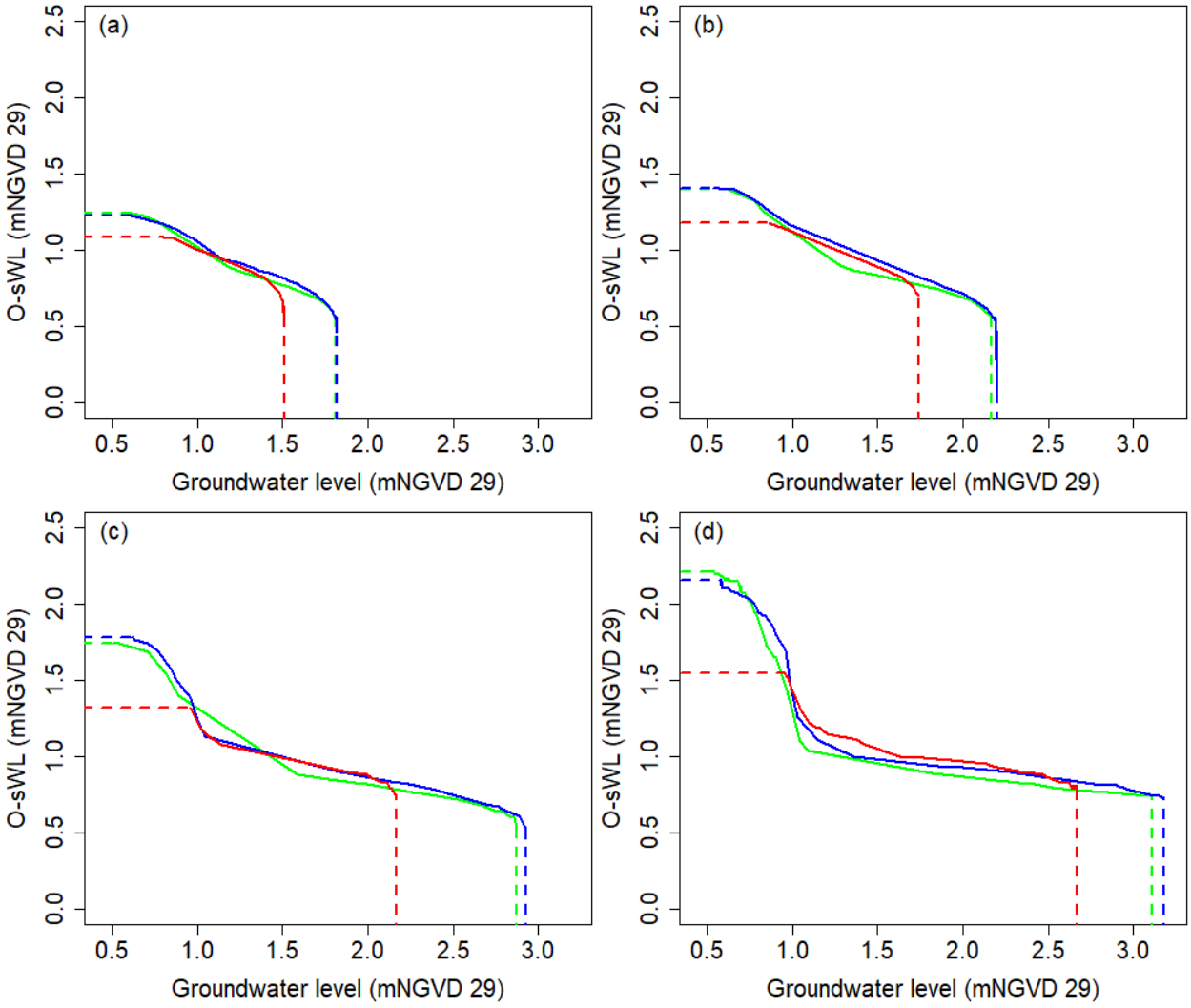

Figure S33: Isolines of O-sWL and groundwater level at Site S22, obtained using the 10,000-year synthetic event records, from the Gaussian copula (blue), Vine copula (green) and HT04 model (red) for return periods of (a) 10-, (b) 20-, (c) 50- and (d) 100-years. Dotted lines represent extrapolation.